THE INFLUENCE OF VERTICAL LOCATION ON HYDRAULIC FRACTURE CONDUCTIVITY IN THE FAYETTEVILLE SHALE

A Thesis

by

KATHRYN ELIZABETH BRIGGS

Submitted to the Office of Graduate and Professional Studies of
Texas A&M University
in partial fulfillment of the requirements for the degree of

MASTER OF SCIENCE

Chair of Committee,	Ding Zhu
Committee Members,	A. Daniel Hill
	Michael Pope
Head of Department,	A. Daniel Hill

May 2014

Major Subject: Petroleum Engineering

ABSTRACT

Hydraulic fracturing is the primary stimulation method within low permeability reservoirs, in particular shale reservoirs. Hydraulic fracturing provides a means for making shale reservoirs commercially viable by inducing and propping fracture networks allowing gas flow to the wellbore. Without a propping agent, the created fracture channels would close due to the in-situ stress and defeat the purpose of creating induced fractures. The fracture network conductivity is directly related to the well productivity; therefore, the oil and gas industry is currently trying to better understand what impacts fracture conductivity.

Shale is a broad term for a fine-grained, detrital rock, composed of silts and clays, which often suggest laminar, fissile structure. This work investigates the difference between two vertical zones in the Fayetteville shale, the FL2 and FL3, by measuring laboratory fracture conductivity along an artificially induced, rough, aligned fracture. Unpropped and low concentration 30/70 mesh proppant experiments were run on samples from both zones. Parameters that were controllable, such as proppant size, concentration and type, were kept consistent between the two zones. In addition to comparing experimental fracture conductivity results, mineral composition, thin sections, and surface roughness scans were evaluated to distinguish differences between the two zones rock properties. To further identify differences between the two zones, 90-day production data was analyzed.

The FL2 consistently recorded higher conductivity values than the FL3 at closure stress up to 3,000 psi. The mineral composition analysis of the FL2 and FL3 samples concluded that although the zones had similar clay content, the FL2 contained more quartz and the FL3 contained more carbonate. Additionally, the FL2 samples were less fissile and had larger surface fragments created along the fracture surface; whereas the FL3 samples had flaky, brittle surface fragments. The FL2 had higher conductivity values at closure stresses up to 3,000 psi due to the rearrangement of bulky surface fragments and larger void spaces created when fragments were removed from the fracture surface.

The conductivity difference between the zones decreases by 25% when low concentration, 0.03 lb/ft^2, 30/70 mesh proppant is placed evenly on the fracture surface. The conductivity difference decrease is less drastic, changing only 7%, when increase the proppant concentration to 0.1 lb/ft^2 30/70 mesh proppant. In conclusion, size and brittleness of surface fracture particles significantly impacts the unpropped and low concentration fracture conductivity.

DEDICATION

I would like to dedicate this work to my parents, Jim and Janna, and my brother, Jamie, for all their support and encouragement as I have pursued my goals in life. Without their love and support I wouldn't have been able to embark on this journey to further my education.

ACKNOWLEDGEMENTS

I would like to thank my committee chair, Dr. Ding Zhu, and my committee members, Dr. Daniel Hill, and Dr. Michael Pope, for their guidance and support throughout the progress of this work. I also would like to thank Dr. Zhu and Dr. Hill for the opportunity to pursue my Master of Science degree in petroleum engineering under their direction and encouragement.

Next, I would like to thank the members within our research group, Junjing Zhang, James Guzek, Tim Jansen and Antony Kamenov. I would also like to acknowledge my friends and colleagues and the department faculty and staff for making my time at Texas A&M University a great experience.

I would like to thank RPSEA for their financial support and Ellington Geologic for providing mineralogical data. I would also like to thank Southwestern Energy for providing the outcrop cores, background information, and production data used in this study.

Finally, thanks to the Department of Petroleum Engineering at Texas A&M University for giving me the opportunity to continue my education and pursue my graduate degree in petroleum engineering.

NOMENCLATURE

h_f	Fracture height (in)
k_f	Fracture permeability (md)
$k_f w_f$	Fracture conductivity (md-ft)
A	Cross-sectional area (in^2)
L	Length over pressure drop (in)
$p1$	Upstream pressure (psi)
$p2$	Downstream pressure (psi)
Δp	Differential pressure over the fracture length (psi)
T	Temperature (K)
W	Mass flow rate (kg/min)
M	Molecular mass (kg/kg mole)
v	Fluid velocity (ft/min)
μ	Fluid Viscosity (cp)
ρ	Fluid density (lbm/ft^3)
z	Gas compressibility factor (dimensionless)
R	Universal gas constant (J/mol K)

TABLE OF CONTENTS

Page

ABSTRACT ii

DEDICATION iv

ACKNOWLEDGEMENTS v

NOMENCLATURE vi

TABLE OF CONTENTS vii

LIST OF FIGURES ix

LIST OF TABLES xii

1. INTRODUCTION 1

    1.1 Hydraulic Fracturing Unconventional Reservoirs 1
    1.2 Fayetteville Shale Overview 4
    1.3 Literature Review 6
    1.4 Problem Description 10
    1.5 Research Objectives 11

2. LABORATORY APPARATUS AND EXPERIMENTAL PROCEDURE 13

    2.1 Description of Laboratory Apparatus 13
    2.2 Experimental Procedure 18
        2.2.1 Core Sample Preparation 19
        2.2.2 Proppant Placement 28
        2.2.3 Fracture Conductivity Measurement 35
        2.2.4 Fracture Conductivity Calculation 41
    2.3 Experimental Design and Conditions 43
        2.3.1 Artificial Fractures 48
        2.3.2 Rock Properties 49
        2.3.3 Field Production Evaluation 50

3. EXPERIMENTAL RESULTS AND DISCUSSION 52

    3.1 Conductivity of Unpropped Fractures 52

3.2 Conductivity of Propped Fractures 55
3.2.1 Conductivity Measurements at 0.03 lb/ft^2 Concentration 58
3.2.2 Conductivity Measurements at 0.1 lb/ft^2 Concentration 60
3.3 Conductivity Analysis 61
3.4 Vertical Zone Variations 68

4. CONCLUSIONS AND RECOMMENDATIONS 77

4.1 Conclusions 77
4.2 Recommendations 79

REFERENCES 81

LIST OF FIGURES

Page

Figure 1 - Location of Fayetteville shale in comparison to Barnett shale location 5

Figure 2 - Evidence of fissility in shale (Glorioso et al., 2012) 8

Figure 3 - Schematic diagram of conductivity laboratory setup 14

Figure 4 - Laboratory setup with major components labelled 15

Figure 5 - Modified API conductivity cell 18

Figure 6 - Experimental process flow process 19

Figure 7 - Shale sample with a rough aligned fracture surface 20

Figure 8 - Shale sample with sandstone cut to height allowing fracture centralization ... 21

Figure 9 - Shale sample glued to sandstone without silicone-base sealant 22

Figure 10 - Aluminum mold used for coating samples in silicone-base sealant 24

Figure 11 - Aluminum mold inner surface 24

Figure 12 - Unpropped FL3 sample 28

Figure 13 – FL3 sample with 0.03 lb/ft^2 30/70 mesh proppant before experiment 29

Figure 14 – FL3 sample with 0.1 lb/ft^2 30/70 mesh proppant before experiment 29

Figure 15 - Application of Teflon tape around the core sample 32

Figure 16 - Hydraulic press sample placement 34

Figure 17 - Fully assemble conductivity cell with flow lines 35

Figure 18 - Conductivity measurement setup 37

Figure 19 - FL2 sample failure prior to experiments 45

Figure 20 - FL3 fracture surface 46
Figure 21 - FL2 fracture surface 46
Figure 22 - Sample work progression flow chart 47
Figure 23 - Aligned fracture schematic 48
Figure 24 - Aligned propped fracture schematic 48
Figure 25 - Unpropped FL3 fracture conductivity 53
Figure 26 - Unpropped FL2 fracture conductivity 54
Figure 27 - Unpropped results from the FL2 and FL3 55
Figure 28 - FL3 sample F02 experimental results 57
Figure 29 - FL2 sample F19 experimental results 57
Figure 30 - low concentration proppant distribution on a FL3 sample 58
Figure 31 - FL3 and FL2 experimental results at 0.03lb/ft^2 59
Figure 32 - FL3 and FL2 conductivity measurements results for 0.1 lb/ft^2 60
Figure 33 - Graphical representation of average fracture conductivity results 61
Figure 34 - FL3 fracture surface particle size 64
Figure 35 - FL2 fracture surface with fragments 64
Figure 36 - FL2 fracture surface particle size 65
Figure 37 - FL2 crushed fracture surface 66
Figure 38 - FL3 crushed sample 67
Figure 39 - Schematic of a typical horizontal wellbore in the Fayetteville shale 69
Figure 40 - FL2 laser profilometer fracture surface scan 72
Figure 41 - FL3 laser profilometer fracture surface scan 73

Figure 42 - FL2 thin section analysis 74

Figure 43 - FL3 thin section analysis 75

LIST OF TABLES

Page

Table 1 - Fracture conductivity calculation parameters 43

Table 2 - Fracture conductivity experimental list 51

Table 3 – Laboratory conductivity measurements 62

Table 4 - Production data anaylsis from the FL2 and FL3 71

Table 5 - Mineralogical data 76

1. INTRODUCTION

1.1 Hydraulic Fracturing Unconventional Reservoirs

Unconventional reservoirs, in particular shale reservoirs, contain large quantities of hydrocarbons trapped within their pore space. However, shale reservoirs are not economical for commercial production because the permeability is too low; therefore, a stimulation technique must be applied to allow gas and oil flow to the wellbore making the wells commercially viable. One of the most common stimulation methods used in shale reservoirs is hydraulic fracturing. Hydraulic fracturing creates highly conductive fractures generating paths for gas and oil to flow. These highly conductive paths increase wellbore communication with the formation by allowing flow from a large surface area.

During a hydraulic fracturing treatment a slick-water or gel liquid is pumped through the wellbore into the formation at a high rate and pressure that exceeds the rock breakdown pressure. Once fractures are created the current practice in industry is to use propping agents to keep the fractures open when pumping has ceased. The amount of propping agent can vary in size, concentration and type, such as natural sand or ceramic grains, depending on the engineer's design specifications. The resulting width of the fracture created by the propping agent, multiplied by the permeability of the fracture results in the conductivity of the fracture. The fracture conductivity is important to industry because it directly relates to the production of wells; therefore, the main goal of hydraulic fracturing is to create and maintain a fracture with substantially greater

conductivity than the formation to increase well production and ultimate recovery (Jones et al., 2009).

Hydraulic fracturing has made important contributions to stimulation of shale reservoirs and has become the most common method to increase hydrocarbon production. In 1947, the first hydraulic fracturing treatment was pumped with gasoline-based napalm-gelled fracturing fluid in the Hugoton gas field on Kelpper Well 1. This was the first well specifically designed to stimulate well production, but by the mid-1960's hydraulic fracturing with water-based fracturing fluid was the primary stimulation method in the Hugoton field (Gidley et al., 1989). Institute of French Petroleum survey reported in 1991, out of all wells completed worldwide, 71% were fracture stimulated (Jones et al., 2009). Additionally, for most operators drilling is the number one expenditure, followed by well stimulation (Jones et al., 2009). For this reason, the oil and gas industry continues to investigate and research what the optimal fracturing fluid, proppant size, concentration and type to cost effectively improve fracturing treatments and still make the most productive wells within diverse formations.

During the early stages of hydraulic fracturing is was common to complete vertical wells resulting in low rate, long production life. Commercial gas production rates were achievable, but it wasn't until the late 1990s when horizontal drilling and multistage hydraulically fractured treatments made the first shale gas play, the Barnett shale, commercially viable. The Barnett shale is estimated to extend over 54,000 sq miles with the Fort Worth basin with thickness ranging from 300 to 500 ft. Prior to 1997 the completion designs consisted primarily of cross-linked gelled fracturing fluid

with large amounts of proppant. These designs resulted in high costs and significant damage to the formation driving the need for completion changes. By the end of 1997, major changes were made to the stimulation design and operators began completing wells with high-rate slick-water fracture treatments. The completion cost of wells was cut approximately 65%, although slick-water treatments did not drastically increase the well production. In 2002, operators began experimenting with horizontal wells that cost twice as much as vertical wells, but resulted in three times the ultimate recovery (Ketter et al., 2008). Success in the Barnett shale has initiated exploration to find other shale plays in which the same completion and stimulation may be used (Matthews et al., 2007).

In 2004, the exploration and completion of wells in the Fayetteville shale began after the wells in the Wedington sandstone were producing considerably higher amounts of natural gas than explainable by conventional analysis. It was determined that the extra production was coming from the Fayetteville shale directly under the Wedington Sandstone reservoir. The Fayetteville shale is an organic-rich shale formation that displays rock and fluid properties similar to the productive Barnett Shale in Texas. Vertical wells were used in the early development of the field to help identify a 300' shale interval and the ideal target zone. The initial completions in the field were nitrogen assisted fracturing fluids, but were soon altered and by the end of 2006 the primary treatments were similar to Barnett shale using slick-water and crosslinked fracturing fluids. Today, slick-water fracturing treatments are the main completion method within the Fayetteville shale field. Sand is used as the propping agent and

65,000 lbs per perforation cluster is required for most treatment designs (Harpel et al., 2012).

Considering the high cost of hydraulic fracturing, the selection of a fracturing fluid and propping agent is significant to well cost and production. The selection of both fracturing fluid and proppant depend significantly on the formation; therefore, understanding how fluids and proppants perform based on rock type, fabric, and mineralogical make-up is invaluable.

1.2 Fayetteville Shale Overview

The Fayetteville shale is an unconventional shale gas play that ranges from Arkansas's western boarder through north central Arkansas. It is Late Mississippian-Chesterian age shale, which is the geological equivalent of the Barnett Shale. The geological description of the Fayetteville shale is black, fissile, concretionary, clay shale with dark-gray, fine-grained limestone inter-bedded within the shale package. The thermal maturity relative to the Barnett shale is higher, confirmed with dry gas production. The total organic content compares favorably with the Barnett shale with total organic content percentages ranging from 4% to 9.5% (Matthews et al., 2007). Below in Figure 1 the location of the Fayetteville in relation to the Barnett shale can be seen.

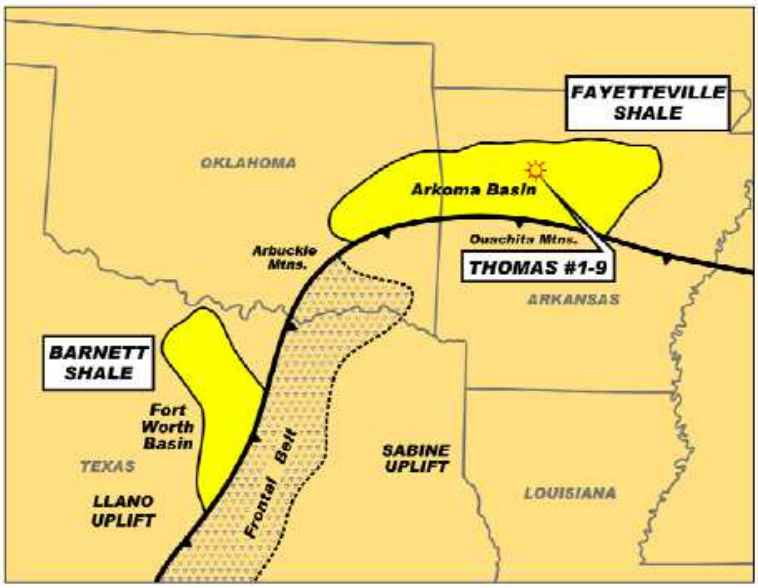

Figure 1 - Location of Fayetteville shale in comparison to Barnett shale location

Currently, Southwestern Energy is the largest operating company in the Fayetteville shale field. Using their formation zone designation there are three main intervals: Upper, Middle and Lower Fayetteville. The Lower Fayetteville is the main area of interest and it is divided into three zones: LFAY, FL2 and FL3. The Lower Fayetteville is the main target subsection. In particular the FL2 has been identified as the ideal target interval because it has the lowest clay content and highest gas porosities with Neutron-Density crossovers indicating good reservoir quality. Throughout the Lower Fayetteville the occurrence of natural fractures with open and filled fracture surfaces has been observed (Harpel et al., 2012).

The fracturing fluid used by Southwestern Energy in a majority of stimulation treatments is slick-water fracturing fluid with the addition of friction reducer, biocides

and scale inhibitor. A typical well in the Fayetteville shale has perforation spacing of 75 feet. The proppant schedule is a combination of 100 and 30/70 mesh sand with fluid volumes averaging 2,500 bbls of fluid per cluster. The average true vertical depth of wells completed in 2010 were 3,727 feet and approximately 3,700 feet was anticipated for wells in 2011 (Harpel et al., 2012).

1.3 Literature Review

Hydraulic fracturing of shale reservoirs is an experimental process that varies from field to field. The variability can be attributed to a number of uncertainties that have the ability to impact the productivity of a well, such as, closure stress, proppant type, proppant grain size and concentration, proppant placement and distribution, rock mechanical properties, gel damage, temperature, non-Darcy and multiphase flow, and residual fracture width. Within the oil and gas industry there has been a strong push to understand how these factors impact conductivity and productivity.

Proppant selection is critical in the design of fracturing treatments and well productivity; therefore within industry it is important to have the ability to consistently compare propping agents. Proppant companies report conductivities of proppant packs to allow operating companies the ability to compare proppant type and size. To experimentally measure the conductivity of proppant packs in a lab the American Petroleum Institute (API) provided industry with standards for measuring short term conductivity in API RP-61 (1989). The recommended procedure is to load 2 lb/ft^2 of proppant uniformly between two metal pistons. Place the metal pistons into a

conductivity cell at ambient temperature and apply a hydraulic pressure for 15 minutes. Pump 2% KCl fluid through the cell at 2 ml/min. and measure the differential pressure and flow rate through the cell giving the values needed to calculate the conductivity. The standards defined in API RP- 61 (1989) are not comparable to actual fracture conductivity due to the variables that impact fracture conductivity that are not accounted for using the API short term conductivity set-up (Palisch et al., 2007).

Measuring the conductivity through a shale fracture is significantly different than measuring the conductivity of a proppant pack on metal pistons or sandstone cores. The rock properties, closure stress, proppant embedment and crushing, gel damage, and residual width are just a few major factors that can impact the reduction of conductivity from that measured by placing proppant on metal pistons. How these variables affect conductivity in shale is an ongoing investigation that gets more complex with every new shale play, primarily due to shale being geologically and mechanically different formation to formation. Identifying variables that significantly impact conductivity remains a focus to further understand how to increase well productivity in shale reservoirs.

Literature has identified mineralogical composition, mechanical properties, and fracture roughness and residual width as important factors of shale conductivity variation. A shale formation is referred to as a fine-grained, detrital rock, composed of silts and clays, which often suggest laminar, fissile structure as shown below in Figure 2.

Figure 2 - Evidence of fissility in shale (Glorioso et al., 2012)

The petrophysical properties of shale can vary greatly often containing different percentages of clay and carbonate, or quartzitic silts. Glorioso et al. (2012) conclude that the principal lithological components of the rock must be determined because they can considerably impact the stimulation design.

Due to the highly variable properties of shale, Palisch et al. (2007) identified reasons it is important to replace the metal pistons required for API RP-61 with reservoir outcrops or reservoir rock. Palisch et al. (2007) identified the major factors occurring downhole causing laboratory conductivity measurements to over predict the in-situ conductivity as proppant embedment, proppant crush, fines migration, cyclic stress, and proppant diagenesis. Non-uniform proppant distribution along the fracture is caused by proppant settlement and formation rock anisotropy. The ductility and clay content of the shale is a major mechanism of proppant embedment; the softer the rock the greater the embedment. Proppant is also affected by edges and corners of non-ideal spherical grains that will be crushed as lower closure stresses; local grains piling up during fracture closing may crush proppant grains at low fracture closure force. Palisch et al. (2007)

also contributes conductivity reduction to fracturing fluid damages, such as, filter cake, gel damage, non-darcy flow, ect.

Hill et al. (2013) performed 88 successful fracture conductivity experiments using Barnett shale outcrop samples. Artificially induced fracture surfaces were created in the real shale outcrop sample in order to perform these experiments. The fracture surfaces were both aligned and displaced. Rock samples used in this experimental process were identified as having infill or no infill in the fracture surface. They identified that fracture surface asperities, rock mechanical properties, proppant embedment and particle migration are factors that impact fracture conductivity. The main mode of comparison in this work was unpropped and propped fracture comparisons by varying proppant sizes and concentrations. The conclusions of this work were that conductivity of hydraulic fractures in shale can accurately be measured in the laboratory, unpropped induced fractures after removal free of particles and debris are conductive, propped fracture conductivity increases with larger proppant size and higher proppant concentration, proppant dominated fracture conductivity declines slower than surface dominated fracture conductivity (Hill et al., 2013).

Investigation of the rock fracture surface has shown that residual fracture widths can be observed from rough fracture surfaces. Van Dam et al. (2001) discuss how the roughness created in the fracture results in residual width after closure. Using a laser profilometer to scan the surface of fractured cement, plaster and diatomite they measured the magnitude of the surface roughness. They concluded that the surface roughness is important for explaining the occurrence of residual width after fracture closure (van

Dam et al., 2001). Mayerhofer et al. (1997) has an agreeable conclusion stating that the residual aperture distribution can be very heterogeneous in all three dimensions forming very conductive fractures.

Currently, there is not a large amount of information published on laboratory experiments using fractured shale cores. Hill et al. (2013) performed successful laboratory fracture conductivity measurements using Barnett shale outcrop samples. Using an appropriate experimental procedure and good control on experimental error allowed for accurate measurements (Hill et al., 2013). The effect of rock mechanics and mineralogical composition of the shale cores used in conductivity experiments is not discussed. This study evaluates two different vertical zones within the Fayetteville shale formation, FL2 and FL3, by comparing experimental conductivity measurements using artificially fractured shale cores. Three different proppant concentrations will be evaluated, as well as rock properties and production data from each zone.

1.4 Problem Description

Hydraulic fracturing treatments account for a large amount of well cost; therefore operating companies are looking for ways to be more efficient by lowering stimulation treatment costs. Each hydraulic fracturing treatment requires tons of proppant, accruing costs from transportation, demand, quality, strength, ect. To evaluate the quantity and type of proppant desired for optimal stimulation design it is key to understand how proppant and shale interact. Fracture conductivity is crucial to well production and is considerably impacted by proppant size, concentration, and type. Conductivity

experiments typically focus on the proppant and not the rock that the proppant is being placed. Literature suggests that the rock properties can vary depending on rock fabric and texture resulting in different interaction between rock and proppant which can significantly impact conductivity.

The Fayetteville shale has an established completion program that uses proppant produced from Arkansas River sand and slick-water fracturing fluid. The formation has multiple geological zones within the 300' shale interval. This study presents the results from a series of conductivity measurements from two different vertical zones, the FL2 and FL3. Outcrop samples were provided by Southwestern Energy. The rock fracture surface created in the Fayetteville shale outcrop cores was artificially induced. The same proppant size and concentrations were used for conductivity measurements to keep consistency between vertical zones. In addition to fracture conductivity measurements, production data from the FL2 and FL3 and rock properties from each vertical zone were compared using thin sections, x-ray diffraction and profilometer surface scans.

1.5 Research Objectives

The main objective of this work was to conduct laboratory measurements of shale fracture conductivity using Fayetteville shale core samples from two different vertical zones. The core samples from FL2 and FL3 vertical locations within the Fayetteville shale formation were tested and compared. Conductivity measurements were determined using the following steps:

1. Implement a reproducible and consistent experimental procedure that allowed the laboratory measurement of static conductivity using Fayetteville shale cores. A modified API RP-61 cell was used in the laboratory procedures.
2. Measure the conductivity of unpropped and propped, induced, rough surface fractures. Vary the proppant concentrations, keeping proppant size and applied closure stresses the same for every experiment.
3. Study the differences in conductivity created by increasing the proppant concentration.
4. Evaluate the effect of vertical changes in a formation on fracture conductivity with and without proppant by comparing the FL2 and FL3 experimental results.

To understand the rock differences between the FL2 and FL3, rock surface scans, x-ray diffraction and thin section analysis will be compared. Moreover, to relate to real world applicability 90-day cumulative production of wells predominately in the FL2 and FL3 will be evaluated.

This work is able to show the difference in fracture conductivity within the same formation, but in different vertical zones. The results of 18 successful experiments establish laboratory results that can be compared for the FL2 and FL3. This study establishes a procedure to evaluate shale core samples using thin sections, x-ray diffraction and a profilometer.

2. LABORATORY APPARATUS AND EXPERIMENTAL PROCEDURE

2.1 Description of Laboratory Apparatus

The American Petroleum Institute developed a standard for proppant conductivity testing documented in API RP-61. The objective of API RP-61 is to unify the experimental design and procedures used in different laboratories. Creating this experimental design provides companies repetitive and reliable results from commercial proppant selection. A more in depth description of the API RP-61 standards can be found in the literature review section of this work.

A modified American Petroleum Institute (API) conductivity cell and procedure was used to perform short-term static fracture conductivity measurements. Fracturing fluid was not used; instead dry nitrogen gas was used to obtain a flow rate. Differential pressure measurements were taken across the fracture surface at different flow rates in order to calculate the conductivity at different closure stresses. The API method uses a smooth fracture surface, whereas for this study Fayetteville cores artificially induced fracture surface was used to simulate a real fracture. Proppant during experiments was placed manually, similar to that of the API RP-61 standards.

The conductivity apparatus for this study consisted of following components necessary for laboratory measurements:

- Hydraulic load frame
- Modified API conductivity cell

- Flow lines
- Two pressure transducers
- Needle valve (back pressure regulator)
- Gas flow controller
- Nitrogen tank
- Data acquisition system

Figure 3 below shows a schematic of how the components listed above are setup in the laboratory (Hill et al., 2013).

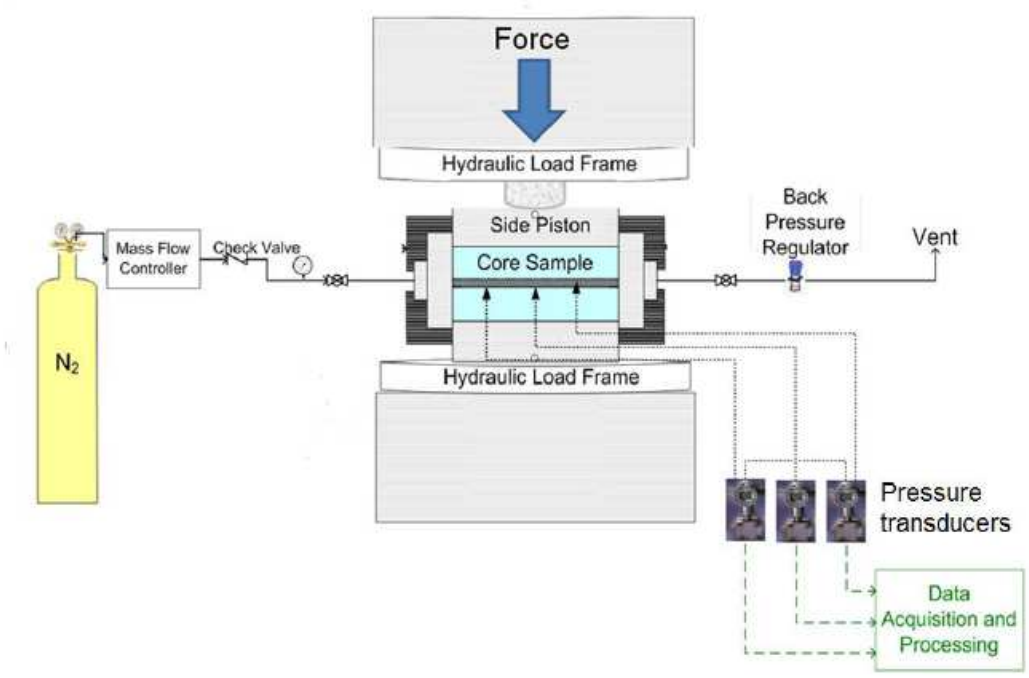

Figure 3 - Schematic diagram of conductivity laboratory setup

Primarily, the main pieces of equipment used to measure conductivity are the nitrogen tank to flow gas, the mass flow controller to control and measure the gas flow rate, the load frame to apply reservoir similar pressures, the two pressure transducers measuring cell and differential pressure, and a back pressure controller to regulate the pressure. The modified API cell, flow lines, and data acquisition system aid in supplying gas, sealing the sample, applying load, and recording measurements. All parts of the setup are crucial to running repeatable experiments. Figure 4 is an image of the laboratory setup used for measuring conductivity with the major equipment labeled.

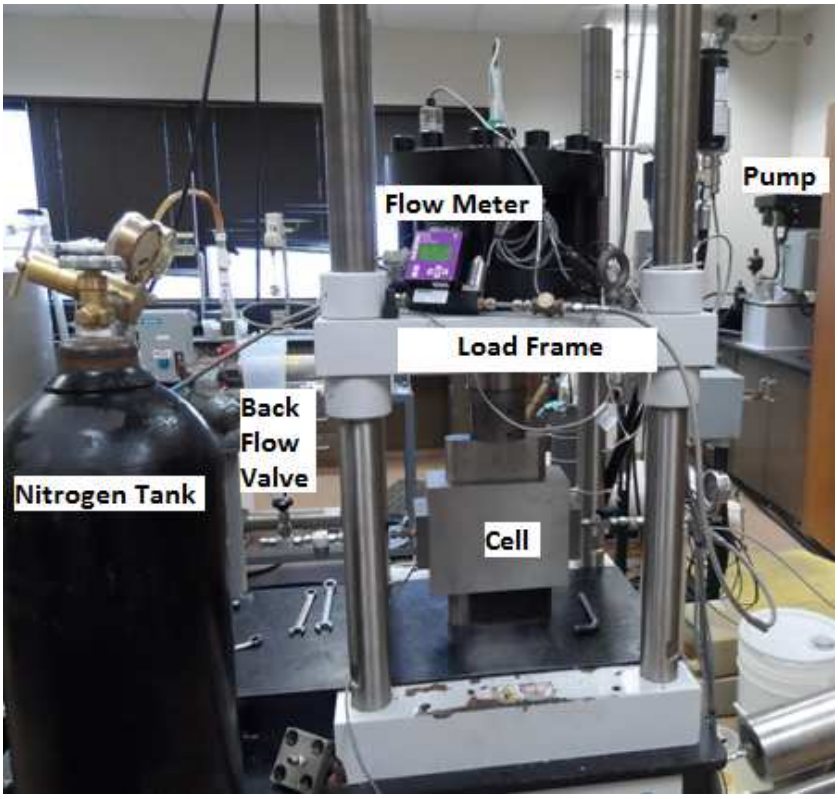

Figure 4 - Laboratory setup with major components labelled

The stainless steel modified API conductivity cell is 10 in. long, 3-1/4 in. wide and 8 in. tall. The cell consists of the cell body, two side pistons and two flow inserts. The cell body is designed to house an epoxy coated sample 7 in. long, 1.65 in. wide, and 6 in. tall, therefore, it is hollowed out with enough tolerance to slide the sample into place. The top and bottom pistons are used to apply stress to the samples. Each piston has a seal that keeps gas from vertically escaping out of the cell if it happens to escape through the epoxy coating. Each piston is 7 in. long, 1.65 in. wide, and 3 in. tall with a hole drilled through the center vertically connecting to a leak-off port. For the Fayetteville shale experiments in this study the leak-off ports were shut in and no leak-off was recorded. The ends of the cell allow for the connection of flow lines using two flow inserts. The inserts have o-rings to seal the cell off from leakage assuring that gas flow is through the fracture.

The nitrogen gas tank is connected to the modified API cell by a series of flow lines. The tank is pressurized up to 2,000 psi and is fully opened during experiments. The control of flow from the tank is done by adjusting a spring valve. The mass flow controller measures the flow rate through the flow line to the cell and is capable of measuring a maximum flow rate of 10 standard liters per minute with an accuracy of 0.001 standard liters per minute.

The hydraulic load frame is rated to apply approximately 16,000 psi of closure stress or 870 kN of force on a piston with surface area of 12 in^2. The piston's axial displacement is recorded by an actuator with accuracy of 0.01 millimeters.

The computer aided testing software controls the load frame and can apply closure stress at a rate of 100 psi per minute as well as record pressure transducer readings.

The two pressure transducers record cell pressure and differential pressure across the fracture. Three pressure measuring ports are located in the middle of one side of the cell, shown below in Figure 5. These ports are drilled through the cell wall to create a path for gas to flow from the sample to the transducers. One transducer measures the cell pressure by attaching to a pressure port in the center of the cell. The other transducer measures the differential pressure from the upstream and downstream pressure ports. The transducers need to be calibrated every six months to make sure they are providing accurate readings because they are an essential part of the conductivity calculation. The transducers selected for this setup can measure pressure with an accuracy of 0.01 psi.

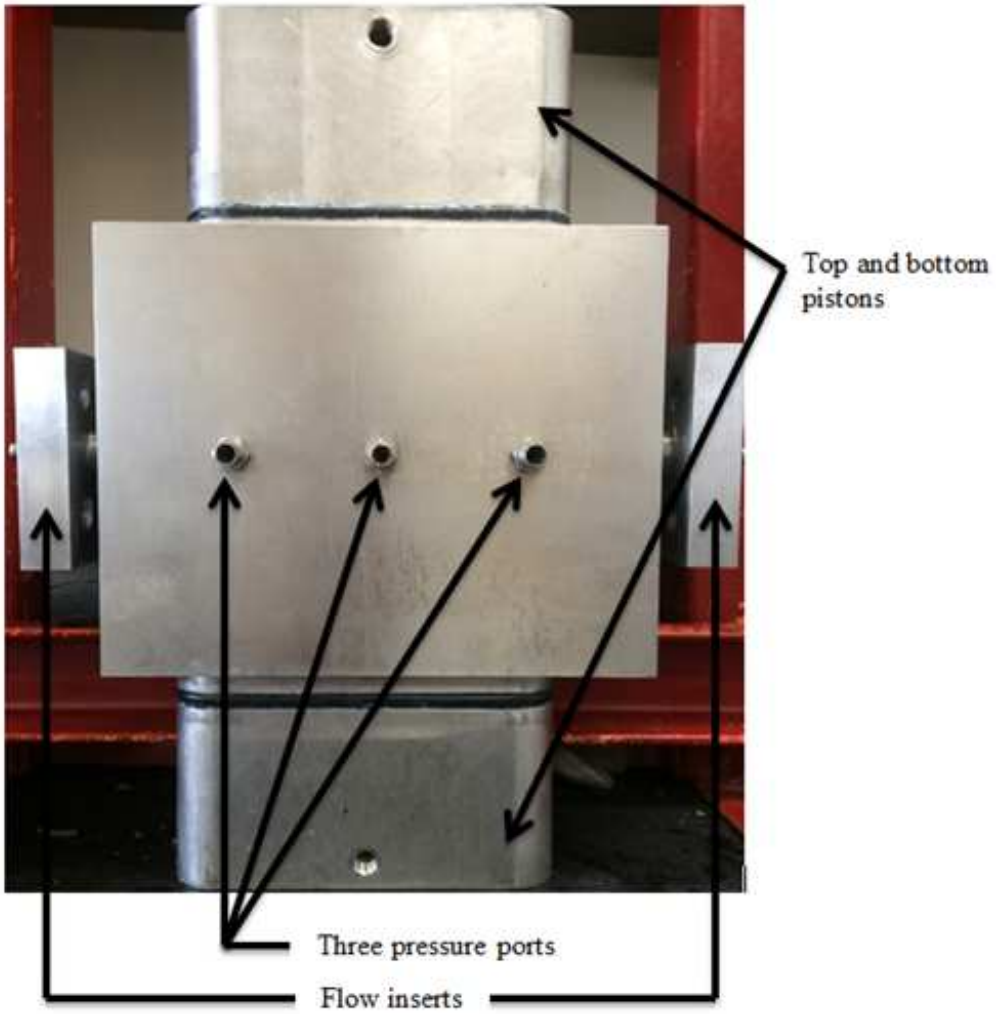

Figure 5 - Modified API conductivity cell

2.2 Experimental Procedure

The experimental procedure used in this work was divided up into three steps: core sample preparation, proppant placement, and conductivity measurement. The procedure was broken up into these three steps to ensure that each core sample was tested under the same conditions. Below is a flow chart of the experimental process:

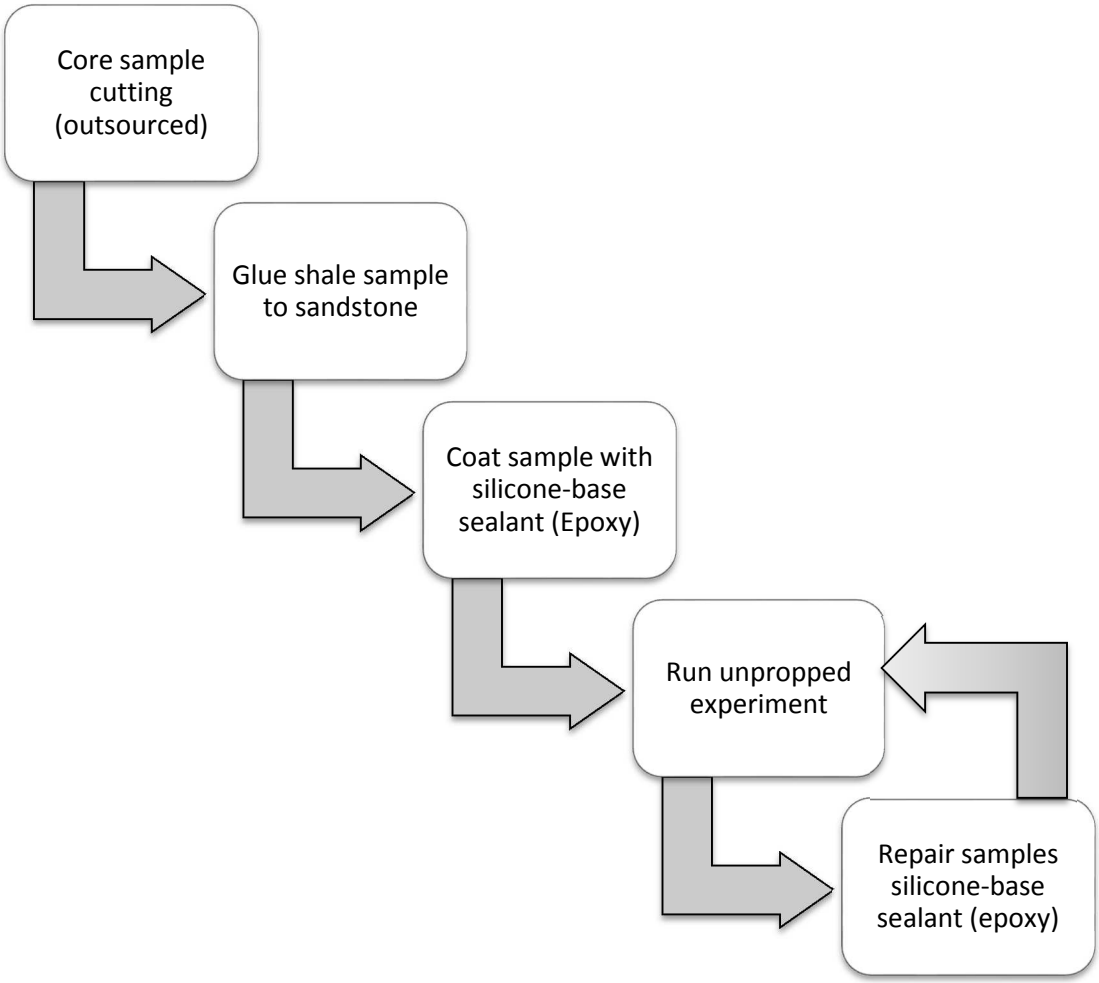

Figure 6 - Experimental process flow process

2.2.1 Core Sample Preparation

Fayetteville shale outcrop cores provided by Southwestern Energy were cut into samples, sized suitable for the aforementioned modified API conductivity cell. Below, in Figure 7, is an example of the shale portion of a sample.

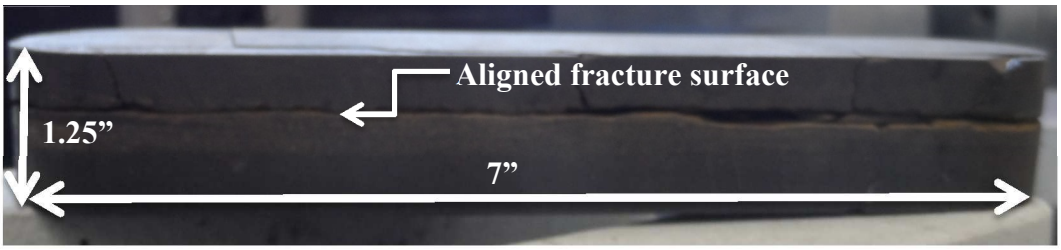

Figure 7 - Shale sample with a rough aligned fracture surface

Working with the Fayetteville shale cores is extremely difficult because it is very brittle in the FL2 and highly laminated in the FL3. To ensure consistency and accuracy of each sample cutting, grinding, and fracture initiation of the shale cores was outsourced. Due to the difficulty handling and cutting the shale, samples vary in thickness from 1 in. to 3 in., however the fracture surface is consistently 1.65 in. wide and 7 in. long. The fractures were artificially created along natural bedding planes to keep the rocks natural fracture surface. When moving the shale portion on the rock sample it is important not to rock, tilt, or vibrate because it can cause surface particles to dislodge and move along the surface.

The additional rock required to make sample height 6 in. was Berea sandstone. The sandstone was cut to the same width and length as the shale but the height of the sandstone halves may vary depending on the height of the shale sample as shown below in Figure 8.

Figure 8 - Shale sample with sandstone cut to height allowing fracture centralization

The sandstone height is directly influenced by the fracture location in the shale sample. The fracture surface on every sample is located approximately 3 in. high in the sample to align with pressure ports and flow inserts. The dimension of a shale sample glued to sandstone is shown below in Figure 9.

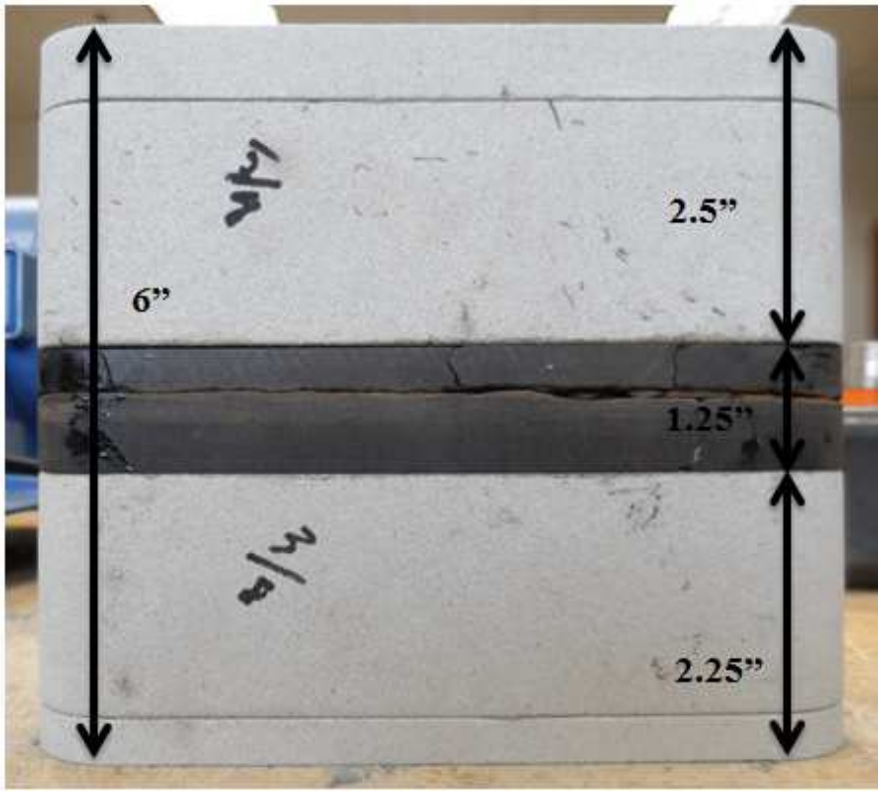

Figure 9 - Shale sample glued to sandstone without silicone-base sealant

Once a sample is glued the fracture is covered with impermeable masking tape to insure that the primer and silicone-base sealant don’t encrouch into the fracture surface. Each sample is labeled on the top and bottom to ensure that the conductivity is always measured in the same direction of flow on the fracture surface from experiment to experiment. The sample is primed for a silicone-base sealant (epoxy). An alumninum mold toleranced, to coat a sample in epoxy while still maintaining the ability to slide into the modified API cell, is used to coat the sample in the epoxy. Step by step procedure for coating a sample in epoxy is outlined below:

1. Tape the fracture of the shale sample to keep the fracture closed during sample preparation and to prevent epoxy from entering the fracture surface. This should be the first thing done before starting the preparation process to keep from opening the fracture prior to running the unpropped experiment.
2. Glue the shale halves to the appropriate sandstone core using Gorilla glue. Be sure to match the correct sandstone half with the matching shale half to ensure that the fracture surface will align with the pressure ports.
3. Apply weight to the glued sample to keep the Gorilla glue from foaming and creating separation between shale and sandstone. Be sure to watch the sample to make sure the shale doesn't slide out of vertical alignment because it will ruin the sample.
4. Remove excess glue emerging from the sides and ends of the sample using a razor blade and sand paper if required. If large quantities of glue are bulging from the sample too much glue was used.
5. Clean residual silicone sealant off of the aluminum mold used for coating the core samples by disassembling the mold. Be sure to clean around screw holes to reduce the possibility of leakage as shown below in Figure 10.

Figure 10 - Aluminum mold used for coating samples in silicone-base sealant

6. Clean the inner surface of the mold with acetone and paper towels to remove any residual materials on the surface as shown below in Figure 11. Do not use any metal tools or materials that will scratch the surface.

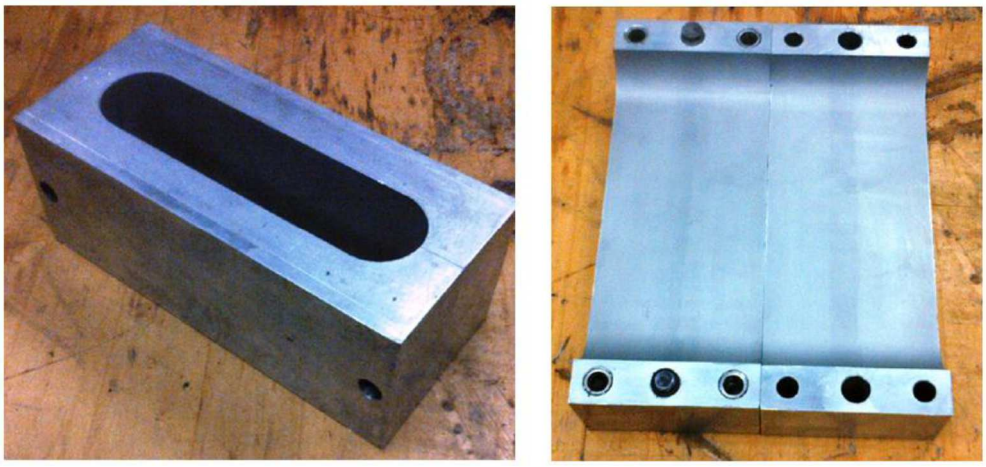

Figure 11 - Aluminum mold inner surface

7. Apply silicone primer with a foam brush to sides of the sample. Examine the fracture tape prior to applying the primer to ensure that the tape is securely adhering to the rock surface. Three coats of the primer are applied with 10 to 15 minute in between each coat.
8. During the down time between primer coats, spray the aluminum mold with silicon mold release agent. Three applications of the spray will be applied to the mold in between each primer coat.
9. First stage of silicone-base sealant: Teflon tape the top of an already prepared core with three wraps of tape and place it in the mold covering 1.5 in. of the mold height. The Teflon tape should create a good seal and prevent leakage through the bottom of the mold. The mold is 3 in. therefore to eliminate the possibility of creating an infinite conductivity path this step is important.
10. First stage of silicone-base sealant: Secure the mold around the previously prepared core by tightening the bolts on the exterior of the mold. Use two wooden blocks 1.5 in. thick to provide support for the mold.
11. Place the sample on top of the previously prepared sample and center it in the mold. Do not touch the surface of the mold with the silicon release agent.
12. First and Last stage: Prepare 40 grams of silicon potting compound and 40 grams of silicon curing agent. Be sure it is always a 1:1 ratio. Stir the mixture well and remove any debris that may have fallen into the mix when pouring. Let the mixture sit until air bubbles can't be seen.

13. Pour the silicon mixture slowly into the mold between the sample and the mold wall. Pour only from one side allowing the mixture to work its way around the entire sample and reduces the chance for air bubbles. Coat the entire surface inside the mold. Tap the outer surface of the mold gently to force any air bubbles trapped inside the epoxy to the surface.
14. Leave the sample at room temperature for an hour. Check for leaks and fluid level decreases. If no leaks are observed place the sample in the oven.
15. Bake the sample in the laboratory oven for three hours at 160°F.
16. Take the mold out of the oven and let it cool down before disassembling the mold. Once the mold has cooled down unscrew the bolts and use a hydraulic jack to remove the sample from the mold.
17. Remove the previously prepared sample used as a spacer from the sample. The previously prepared sample is no longer needed for stages two and three.
18. Use a razor cutter to cut extra epoxy and straighten the edge prepared. This will create a smooth edge between stage one and two for the epoxy to adhere together.
19. Stage two: repeat mold cleaning process from stage one. Prime sample and wrap three layers of Teflon tape around the first stage epoxy and assemble the mold around the top of the first stage using 1 in. wooden blocks. Prepare 50 grams of silicon potting compound and 50 grams of silicon curing agent for this stage. This stage should coat the fracture surface and provide a solid layer of epoxy that does not allow for any infinitely conductive paths.

20. Stage three: clean and prepare mold the same as stages one and two. Wrap three layers of Teflon tape around the top of the second stage epoxy coating. Place a previously prepared sample underneath each mold half and bolt the mold together around the sample. The remaining portion of the sample should be inside the mold. Prepare 40 grams of silicon potting compound and 50 grams of silicon curing agent. Quantity of silicon mixture may vary slightly based on the remaining sample left to cover.
21. Remove any epoxy that may have accumulated on the top of bottom of the sample.
22. Using a razor cutter, cut three windows in the epoxy for pressure port readings. The windows allow access from the fracture to the differential pressure transducer and the cell pressure transducer.
23. Cut a window approximately 3 in. high in both ends of the sample to allow flow through the sample from the flow inserts.
24. For unpropped experiments, the sample is ready to be prepared for experimental use.
25. For propped experiments, the fracture must be opened using a razor cutter to follow the fracture surface. Separating the two surface can often be challenging because the surface is so rough and varies in height; therefore, be very careful because if cut incorrectly sample may be ruined and need to be re-prepared. Once the epoxy has been cut and the fracture is open, place the proppant as desired and close fracture.

2.2.2 Proppant Placement

The proppant used for the experiments in this study were provided from Southwestern Energy's sand plant. The 30/70 mesh Arkansas River sand from the sand plant is identical to what is pumped during fracturing treatments within the Fayetteville shale.

Proppants were evenly distributed on the fracture surface manually before each propped experiment. Below in Figure 12 is the rough fracture surface of an FL3 sample. This sample has already been experimentally tested for unpropped conductivity but this image is prior to manually placing proppant.

Figure 12 - Unpropped FL3 sample

Figure 13 and Figure 14 show an example of the distribution of 30/70 mesh proppant at 0.03 lb/ft^2 and 0.1 lb/ft^2 concentrations, respectively.

Figure 13 – FL3 sample with 0.03 lb/ft^2 30/70 mesh proppant before experiment

Figure 14 – FL3 sample with 0.1 lb/ft^2 30/70 mesh proppant before experiment

The steps for proppant placement on the fracture surface are as follows:

1. Wrap two rows of Teflon tape around the bottom and top half of the sample. Each row will be wrapped with three layers of tape. The placement of the lower row on the bottom half of the sample shouldn't be too close the bottom of the sample otherwise placement into the cell will be difficult.
2. Measure desired proppant concentration on an electronic scale using the following equation to calculate the lb/ft^2.

$$\frac{lb}{ft^2} = \frac{(weight\ grams\ measured\ on\ scale)x\ 0.0022}{(Area\ of\ Sample\ 12in^2)/144}$$

Where

3.2 grams = 0.0847 lb/ft^2 ≈ 0.1 lb/ft^2

1 gram = 0.0264 lb/ft^2 ≈ 0.03 lb/ft^2

3. Place the sample on a piece of 8.5 in. by 11 in. paper. The paper allows for easier movement of the sample by reducing the friction of the epoxy on the table or surface it is sitting on. This will allow easier rotation of the sample when applying the Teflon tape in step 6 below. Be sure to place the sample on the paper prior to placing proppant because moving the sample after proppant placement can risk rearrangement of proppants.
4. Place proppant on the bottom half of the sample, evenly distributing it on the surface.

5. Place the top of the sample on the bottom being sure not to disturb any of the proppant placed on the fracture surface. The easiest way to place the top of the sample on the propped fracture is by aligning the pressure port and flow insert windows.
6. Wrap three layers of Teflon tape in two columns perpendicular to the fracture, between the pressure ports. Be careful not to apply to much pressure on either half of the sample as it will separate the fracture and move proppant. The Teflon tape columns will reduce the chance of gas migration or leakage in the horizontal direction.
7. Apply high-pressure vacuum grease to each row and column of Teflon tape allowing the sample to slide into the cell and providing a seal between the sample and the cell walls. The grease is critical to sample placement because it places the sample without damaging the epoxy coating or the modified API conductivity cell walls. Figure 15 shows the placement of Teflon tape around a sample in relation to cell pressure port locations.

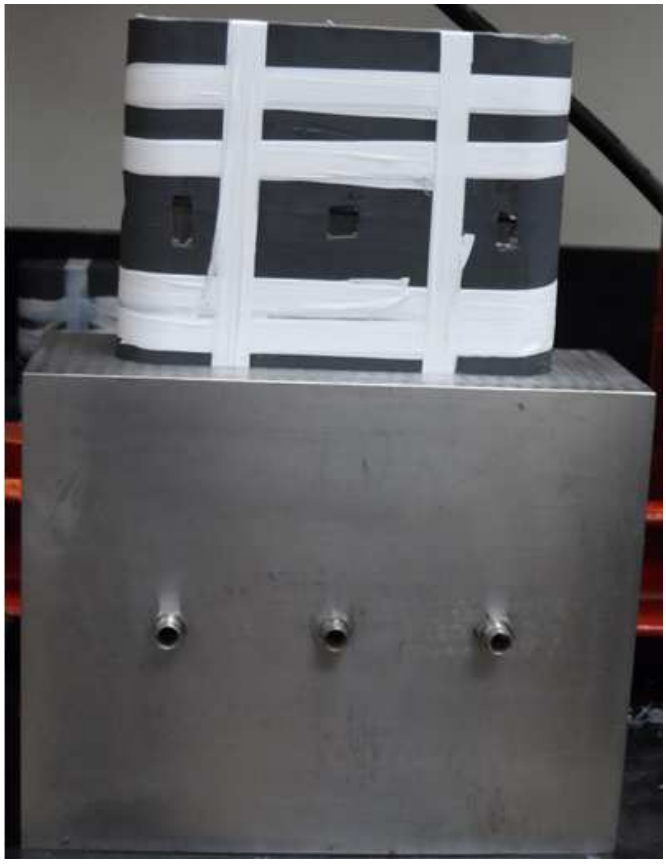

Figure 15 - Application of Teflon tape around the core sample

8. Press the wrapped sample into the modified API conductivity cell using a manual hydraulic press.
9. Align the fracture in the center of the conductivity cell using the flow insert windows as guides.
10. Carefully, lift the cell and place it on top of the bottom piston, making sure not to tilt or shake the cell displacing proppant. O-rings on the top and bottom pistons provide a good seal, but need to be coated with high-temperature o-ring grease to prevent wear and tear.

11. Plug the leak-off port on the bottom piston using a threaded bolt. The threads should be wrapped with three layers of Teflon tape to provide a good seal.
12. Carefully, move the conductivity cell to the load frame. Do not rock or tilt the cell or proppants may be rearranged resulting in inaccurate conductivity results.
13. Place the top piston into the conductivity cell.
14. Center the cell in the load frame.
15. Turn on the GCTS control box and wait till the red interlock light turns off and the green control light illuminates.
16. Open the CATS software program and turn on the pump.
17. Using the software execution files apply a 500 psi closure stress at 100 psi per minute increments.
18. After 500 psi closure stress is applied attach the flow inserts into the ends of the conductivity cell and attach all flow lines and transducers.
19. Plug the leak-off port on the top piston similarly to plugging the bottom piston. This will keep any gas from escaping through the leak-off ports.

Figure 16 shows the manual hydraulic press used to place samples into the modified API conductivity cell. The flow direction and pressure port locations are marked showing the direction of flow. The differential pressure transducer reads the pressure difference between ports labeled T3 and T1 in Figure 16. The cell pressure transducer reads the pressure from the pressure port labeled T2.

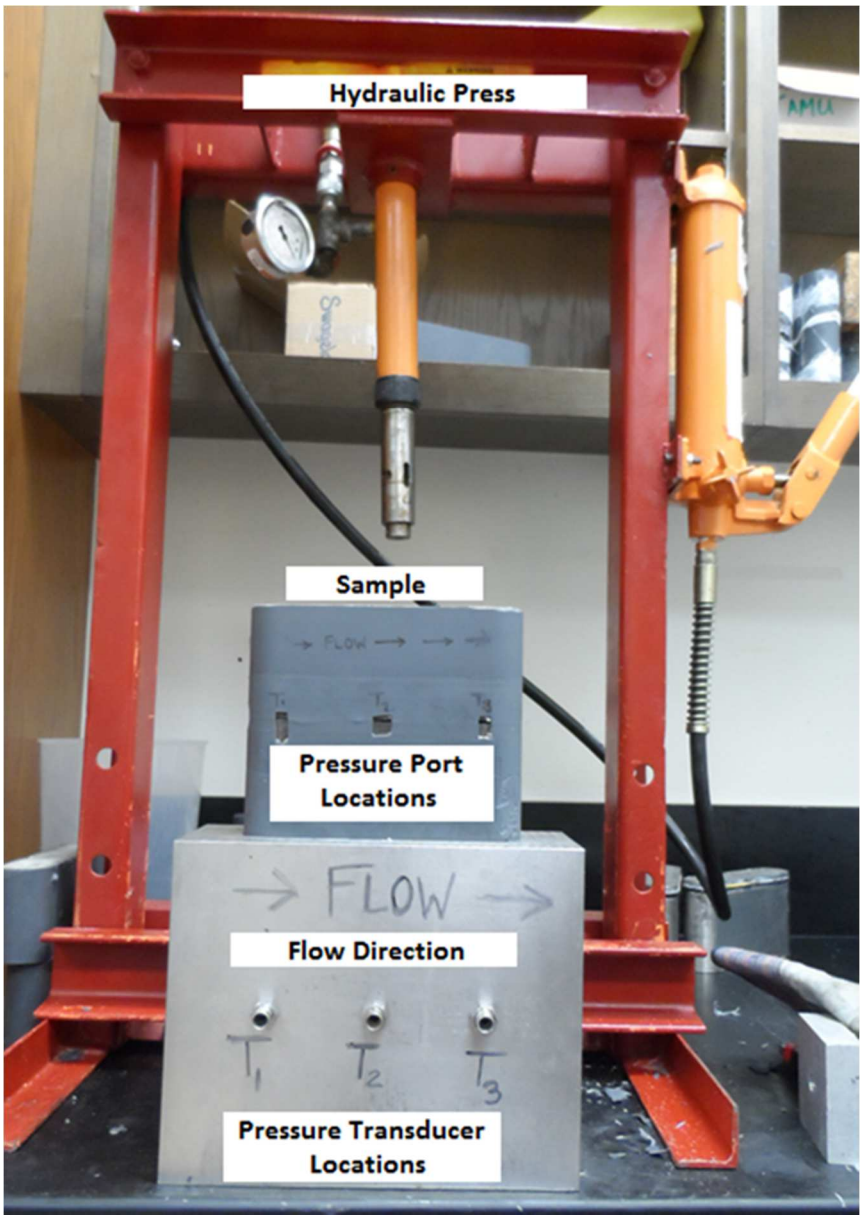

Figure 16 - Hydraulic press sample placement

Figure 17 shows the fully assembled system from the pressure port side of the cell.

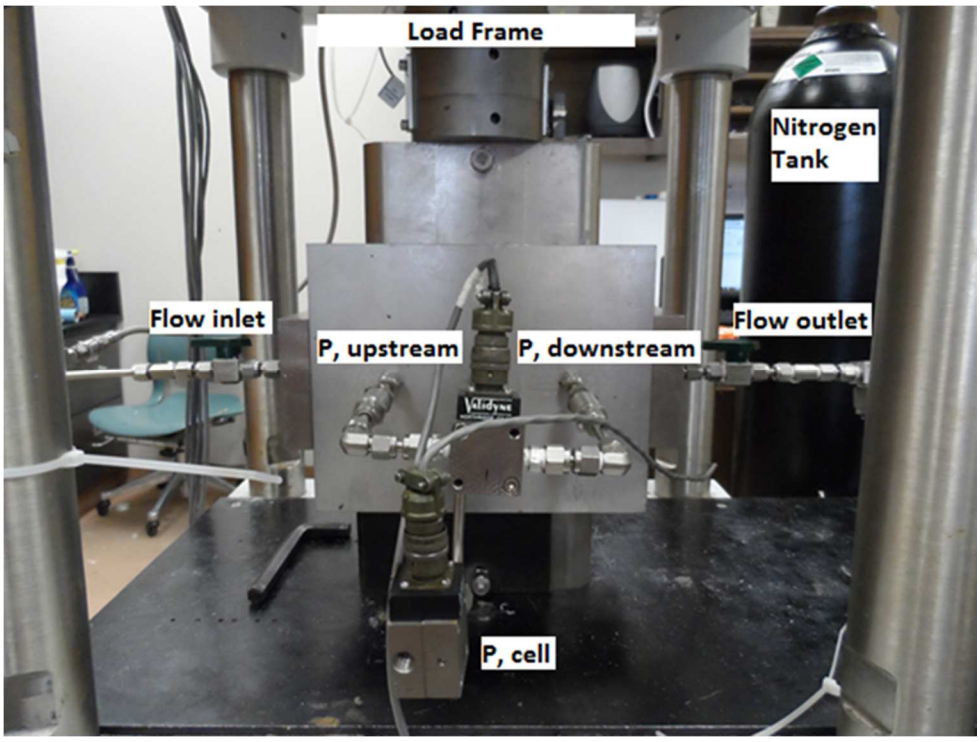

Figure 17 - Fully assemble conductivity cell with flow lines

2.2.3 Fracture Conductivity Measurement

The primary focus of this work was to measure the short-term fracture conductivity measurements and compare the results from the FL3 and to the FL2. To simulate the dry gas being produced through fractures in the Fayetteville shale field dry nitrogen gas was used. Laboratory conductivity measurements were measured at room temperature in the same lab using the same setup for each experiment. Conductivity was measured by recording the dry nitrogen gas flow rate on the flow meter and the differential pressure across the fracture at four different closure stresses. The closure stresses selected for this work were 500 psi, 1,000 psi, 2,000 psi, and 3,000psi. The final

closure stress was selected to be 3,000 psi because the average in-situ stress gradient in the FL2 and FL3 zones is 0.7 to 0.75 psi/ft. In 2011, it was anticipated that the average true vertical depth would approximately be 3,700 feet providing evidence that 3,000 psi closure stress in the lab is comparable to the stresses observed in the field (Harpel et al., 2012). The conductivity at each closure stress was calculated using Darcy's law based the four data points collected at varying flow rates. The laboratory conductivity measurement procedure starting from the end of the procedure listed in section 2.2.2 is detailed below:

1. Plug the mass flow controller in and allow it to self-calibrate. The flow rate display will stabilize when it is ready for use.
2. Close the back pressure regulator at the outlet of the conductivity cell to ensure no gas should flow out of the cell once gas is flowing from the nitrogen tank.
3. Check the mass flow controller reading and record the baseline flow rate before gas is introduced to the system.
4. Open the spring valve connected to the nitrogen tank completely by turning the knob to the left. This prevents the gas from flowing through the flow lines when the gas tank is opened.
5. Turn the valve on the nitrogen tank to open. The gas should be trapped between the tank outlet and the spring valve ensuring that gas is not flowing through the flow lines. The spring valve is used to control the amount of gas flowing into the system.

6. Turn the spring valve slowly to the right to start the flow of nitrogen into the cell. The spring valve is extremely sensitive and will increase flow by barely turning the valve. The cell pressure should be increased and stabilized at 50-55 psi. When adjusting the spring valve pay close attention to the flow rate meter, it should not exceed 1.5 standard liters per minute. If the flow rate exceeds this flow the proppant is at a high risk to rearrange inside the fracture due to the low closure stress. Below in Figure 18 the spring valve, mass flow controller and nitrogen tank discussed in steps 1-6 are shown.

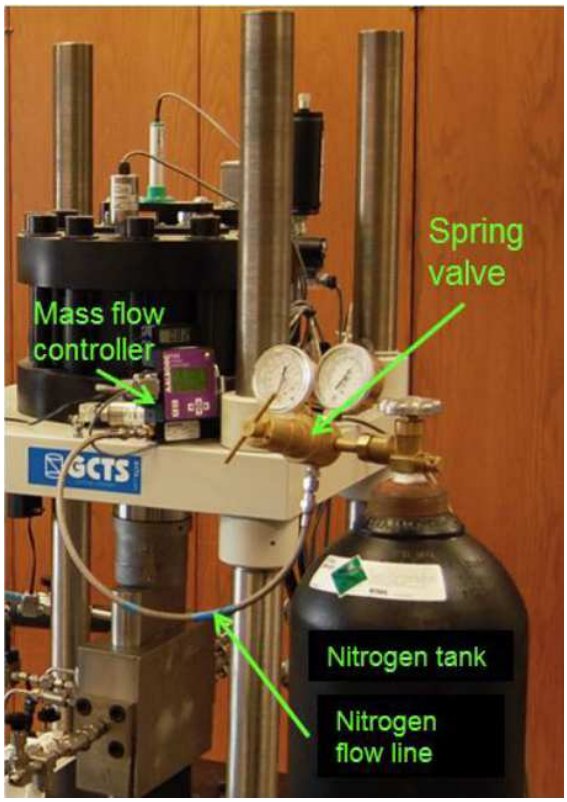

Figure 18 - Conductivity measurement setup

7. Stabilize the cell pressure for approximately 15 minutes or until the differential pressure transducer stabilizes. If the cell does not hold pressure there is leakage in the system. The mass flow rate should stabilize at the base line flow rate recorded in step 2 there, if it does not there is leakage in the system. If there is leakage in the system the experiment must be stopped because the conductivity measurements will be abnormally high.
8. Open the back pressure regulator allowing flow through the system. Starting flow through the system often results in a slight spike in flow, so carefully increase the gas flow rate.
9. Record the differential pressure, flow rate, and cell pressure once the cell pressure and differential pressure have stabilized. Exceeding a flow rate of 1.0 liter per minute can increase the possibility of turbulent flow and non-Darcy flow; therefore, try to avoid flow rates greater than 1.0 psi.
10. Change the flow rate by opening the back pressure regulator more. The back pressure regulator needs to be opened enough to increase the differential pressure by 0.03 psi. Also, the differential pressure shouldn't exceed 10% of the cell pressure because gas is highly compressible.
11. Repeat step 10 two more times to get a total of four measurements for 500 psi closure stress.
12. Close the back pressure regulator and export the data.

13. Increase the closure stress to 1,000 psi at a rate of 100 psi per minute. An execution file is set up within the CATS software to consistently apply the same setting. Open the back pressure regulator slightly during this process to avoid any excessive gas pressure build up in the fracture while increase the closure stress.
14. Once 1,000 psi closure stress has been applied close the back pressure regulator and monitor the cell pressure. Cell pressure should be between 50-55 psi.
15. Repeat steps 7-12 to record values for conductivity measurements at 1,000 psi closure stress. Using the same or close flow rates is suggested, but due to differential pressure this may not always be possible.
16. Repeat 7-14 for 2,000 and 3,000 psi closure stresses.
17. After all measurements have been recorded the experiment is finished and the apparatus must be carefully taken apart.
18. Close the nitrogen tank and open the spring valve so there is no flow into the system.
19. Open the back pressure regulator allowing the remaining gas in the system to flow through. The flow meter should be monitored during this process to not exceed 2-3 liters per minute. Additionally, the differential pressure and cell pressure need to be monitor to not safely stay below the limits of the transducers approximately 5 psi and 65 psi respectively are suggested.
20. Close the valve at the entrance of the cell and open the bypass valve to bleed off the gas trapped in the spring valve.

21. Slowly turn the spring valve to release the gas trapped. Be sure the nitrogen tank has already been closed as stated in step 18.
22. Disconnect all flow lines, pressure transducer lines, flow inserts and plug in the top cell piston. The load should still be applied to the cell to make it easier to disconnect the flow lines and remove the inserts.
23. Reduce the closure stress using the axial displacement setting in the CATS software. Lift the top piston of the load frame until there is space between the cell and the piston. This will allow the ability to slide the cell out from the load frame.
24. Shut down the pump and system controller. The controller should switch to interlock before manually switching it to the off position.
25. Unplug the flow rate controller from the electrical outlet.
26. Remove the top piston from the cell.
27. Move the cell to the hydraulic press.
28. Remove the plug from the bottom piston.
29. Place the cell into the hydraulic press and apply stress to the sample. The bottom piston will need a slight force to remove. Monitor the flow insert windows to minimize the amount of epoxy pealing when removing the sample.
30. Clean the cell using a degreaser and paper towels.

2.2.4 Fracture Conductivity Calculation

The differential pressure, flow rate, and cell pressure measurements recorded during the fracture conductivity experiments are needed to calculate the conductivity at the four closure stresses. To calculate the conductivity of the propped and unpropped fractures in this work three equations were needed, Darcy's law, the real gas law and gas flux, given below:

Darcy's law

$$\frac{-dp}{dL} = \frac{\mu v}{k} \tag{2-1}$$

Real gas law

$$\rho = \frac{pM}{zRT} \tag{2-2}$$

Gas flux

$$\frac{W}{A} = \rho v \tag{2-3}$$

Multiplying Darcy's law by the fluid density, ρ, and rearranging to get *dp* and *dL* on opposite sides gives the following equation:

$$\rho(dp) = \frac{\mu v}{k}\rho(dL) \tag{2-4}$$

The real gas law is a function of pressure, *p*, in order to get *ρ* as a function of the length between differential pressure ports, *L*, the gas flux equation (2-3) must be rearranged as shown below:

$$\rho = \frac{W}{Av} \tag{2-5}$$

Substituting the density equation 2-5 into equation 2-4 yields,

$$\frac{pM}{zRT}dp = \frac{\mu v}{k}\frac{W}{Av}dL \tag{2-6}$$

Simplifying to,

$$\frac{pM}{zRT}dp = \frac{\mu}{k}\frac{W}{A}dL \tag{2-7}$$

Integrating equation 2-7

$$\frac{M}{zRT}\frac{({p_1}^2-{p_2}^2)}{2} = \frac{\mu L}{k_f}\frac{W}{A} \tag{2-8}$$

The gas velocity in the fracture is equivalent to $\frac{q}{w_f h_f}$, therefore the $\frac{W}{A}$ equation becomes,

$$\frac{W}{A} = \frac{q\rho}{w_f h_f} \tag{2-9}$$

Plugging equation 2-9 into equation 2-8 yields:

$$\frac{M}{zRTL}\frac{({p_1}^2-{p_2}^2)}{2} = \frac{\mu q\rho}{h_f}\frac{1}{w_f k_f} \tag{2-10}$$

Evaluating equation (2-10) using the slope intercept formula, $y = mx + b$, where the left side of equation (2-10) is plotted on the y-axis and $\frac{\mu q\rho}{h_f}$, from the right side of equation 2-10, is plotted on the x-axis. The slope of the line is equivalent to the inverse of fracture conductivity, $k_f w_f$, where, k_f is fracture conductivity and w_f is fracture width after closure.

A list of all parameters used to calculate fracture conductivity can be found below in

Table 1.

Table 1 - Fracture conductivity calculation parameters

Differential pressure	Δp	measured	psi
Flow rate	q	measured	Liter/min
Atmospheric pressure	P_{SC}	14.7	psi
Universal gas constant	R	8.3144	J/mol-K
Compressibility factor		z	1.00
Temperature	T	293.15	K
Fracture Lengths	Lf	5.25	in.
Fracture width	hf	1.65	in.
Density of nitrogen	ρ	1.16085	kg/m3
Viscosity of nitrogen	μ	1.7592E-05	Pa·s
Molecular mass of nitrogen	M	0.028	kg/mole

2.3 Experimental Design and Conditions

Southwestern Energy is the largest operator in the Fayetteville shale; therefore, their current completion treatment design was analyzed and the same proppant used in the field was selected for the experimental work in this study. Currently, the completion treatments consist of slickwater fracturing fluid mixed with a few additives and low proppant concentrations. Proppant for the fracturing treatments is predominately provided by Southwestern Energy's sand plant, which provides 100 and 30/70 mesh sand. The 100 mesh sand is pumped at low concentrations at the beginning of the job followed by the larger mesh size, 30/70. The tail end of the treatment has slightly higher proppant concentration to ensure near well-bore fracture conductivity. For this

experimental study 100 mesh sand was not examined because it accounts for a small volume of proppant pumped during the fracturing treatment; therefore, 30/70 mesh sand will be examined at low concentrations.

Drilling aims to place the wellbore in the FL2 although due to geological variation the wellbore can often end up within the FL3 which is found directly below the FL2. Faulting and other stratigraphic features also play a role in the variation across the field in Arkansas. Additionally, formation heterogeneity can cause differences in fracture surface roughness, mineralogical content and overall rock fabric that can impact fracture growth and complexity (Ispas et al., 2013). For this reason, the rock property differences between the two zones were compared to interpret how their laboratory conductivity measurements would differ.

Sample fracture surfaces for this work were artificially induced, aligned fractures. The fracturing and cutting method of the samples was the same for every outcrop block cut, but the FL2 and FL3 behaved differently causing fewer samples to be made in the FL2 zone. The main cause for this anomaly was the rocks fracture network. The FL2 created more complex fractures sometimes consisting of fracture growth perpendicular to the fracture surface therefore ruining the sample. The FL3 on the other hand fractured primarily on the bedding plane, parallel to the fracture surface which allowed better control when cutting and grinding the samples edges. The main goal of this work was to analyze the fracture conductivity measurements from the FL2 and FL3. Maintaining the samples surface integrity and using the same proppant size and concentration for experiments in both zones was the key to this study. Figure 19 below

shows the surface of an FL2 sample that had been crushed during initial fracturing. This particular sample failed before the sample was ever used for experimental fracture conductivity experiments because of a fracture that penetrated the entire surface of the fracture compromising the integrity of the sample. The crushed rock pieces were placed on the surface to show how FL2 samples break and loose fragments are created.

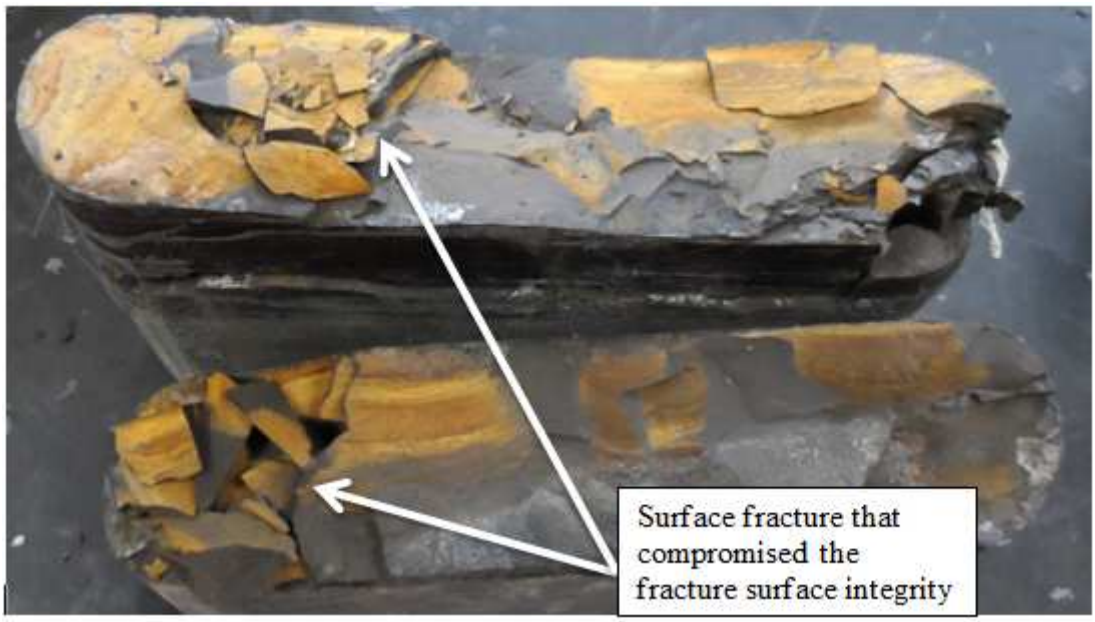

Figure 19 - FL2 sample failure prior to experiments

A typical fracture surface for a sample in the FL3 and FL2 can be seen in Figure 20 and Figure 21, respectively.

Figure 20 - FL3 fracture surface

Figure 21 - FL2 fracture surface

Three conductivity experiments were run on three samples from the FL2 and three samples from the FL3: unpropped, 0.03 and 0.1 lb/ft^2. The finer 100 mesh sand was used to evaluate the impact of proppant concentration using two samples from the FL3. Laboratory conductivity measurements that required high flow rates in order to create a differential pressure drop increase the possibility of error in the conductivity calculation with Darcy's law.

The rock fabric and texture of each zone was used to help identify difference between the two vertical zones by using thin section, x-ray diffraction, and profilometer

surface scan analysis. A work flow diagram of a typical sample's experimental process can be seen below:

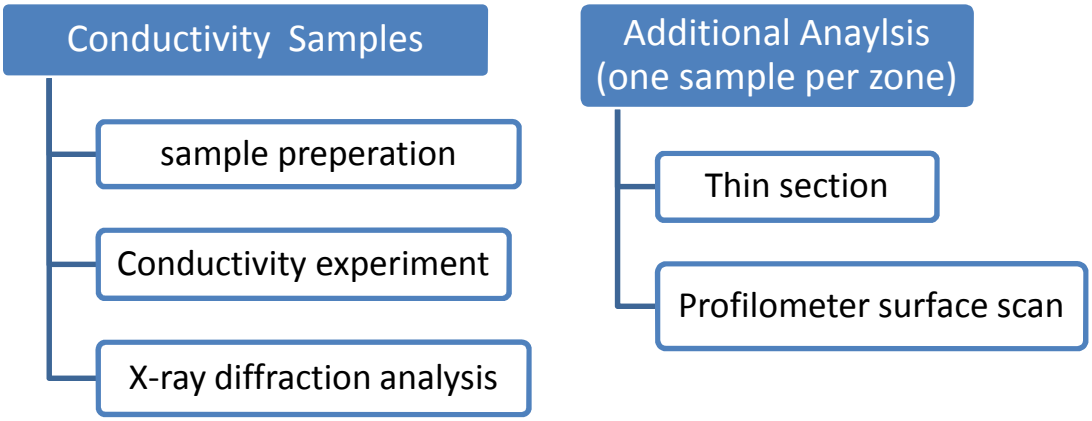

Figure 22 - Sample work progression flow chart

Finally, field data was used to analyze wells that have 100% of their wellbore in the FL2 and the FL3. The combination of total organic carbon content and gas porosity of the FL2 makes it the ideal target interval within the Fayetteville shale, but the total organic carbon content of the FL3 and FL2 do not vary greatly. The FL2 total organic content ranges from 2.5% to 7.5%, whereas the FL3 ranges from 3.5% to 6% (Harpel et al., 2012). Many operating companies look to optimize the production from shale reservoirs by determining the best location for well placement, perforation, and hydraulic fracturing. The most favorable zone within a shale formation is the one with the highest hydrocarbon potential and flow capacity. The highest hydrocarbon potential is based on four different petrophysical terms gas porosity, water saturation, total organic carbon content, and kerogen type and thermal maturity (Torres-Verdin et al.,

2013). This study will analyze the production data and compare to experimental conductivity results from each zone, understanding that slight differences between these two zones in terms of petrophysical data may be seen.

2.3.1 Artificial Fractures

Fracture surfaces were created by artificially fracturing the core samples along natural bedding planes. Fractures were left closed till propped testing to retain any surface fragments and roughness disparities. A schematic of the aligned fracture surface can be seen in Figure 23.

Figure 23 - Aligned fracture schematic

Each aligned fracture was opened after the unpropped fracture conductivity experiment. During this process some surface fragments were lost on some samples. Proppant placement on the FL2 and FL3 samples was done manually resulting in propped surfaces similar to the schematic shown in Figure 24.

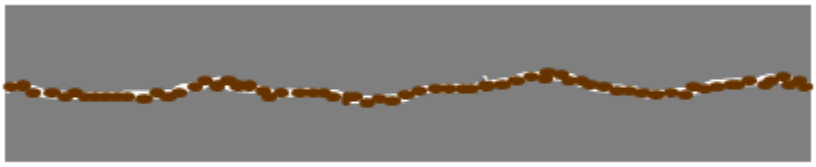

Figure 24 - Aligned propped fracture schematic

The key focus of this study was to investigate the conductivity differences between the FL2 and FL3 zones using the same artificial fracturing method, proppant size and concentration.

2.3.2 Rock Properties

Evaluation of the FL2 and FL3 rock properties was used to show differences between the two zones. The FL3 was highly laminated and had very smooth surfaces relative to the surfaces observed in the FL2 samples. The surface of the FL2 was dominated by peaks and valleys that were not present in the FL3. For this reason a laser profilometer was used to scan the surface of one sample from each zone prior to experimental test.

Additionally, the FL2 and FL3 were defined by Southwestern Energy as two different geological zones within the same formation. To shed light on how these two zones vary geologically the mineralogical content was evaluated. The mineralogical content variation was particularly of interest to see how it impacted conductivity. Proppant rock interaction is a huge part of conductivity because if a proppant is too hard it will embed into the surface and if a proppant is too soft it will crush (Palisch et al., 2007). Rock properties play a large role in fracture complexity; therefore, mineralogical content is a significant factor in fracture complexity (Ispas et al., 2013). For this reason, x-ray diffraction analysis was performed on samples from the FL2 and FL3 to evaluate differences in the two zones.

Lastly, rock properties were evaluated using thin section analysis. Thin sections analysis, particle sieving techniques and laser diffraction are all methods traditionally used to describe a rocks texture. Facies analysis and environmental deposition interpretation can provide information about grain size and shape by describing the rock fabric and texture. Furthermore, rock fabric and texture can help identify the sand strength and failure, critical to production and completion engineers when designing hydraulic fracturing treatments (Knackstedt et al., 2005). For this study thin section will be used to evaluate grain size and natural fracture orientation differences.

2.3.3 Field Production Evaluation

To relate this study to field production Southwestern Energy provided 90-day cumulative production data from ten different wells, four FL3 wells and six FL2 wells. In order to reduce the chances of large petrophysical differences only wells on the same well pad were selected for this evaluation. The wells compared were typically drilled in the same planer direction, North-South or East-West.

Laboratory conductivity measurements were compared to production data to investigate if laboratory differences correlated to field data. Production data was normalized by the total number of perforations in the entire wellbore. Analysis of this data is important because it could give insight in terms of what to expect from the FL2 and FL3 conductivity experiments. Production data could also provide support to the findings in this work, because production is greatly dependent on conductivity of fractures.

Below in Table 2 shows a list of experiments run for the FL2 and FL3 zones.

Table 2 - Fracture conductivity experimental list

	Number of Conductivity Experiments 30/70 mesh sand			
Fracture Zone	***Unpropped***	***0.03 lb/ft²***	***0.1 lb/ft²***	***Total***
FL2	3	3	3	9
FL3	3	3	3	9
				18

3. EXPERIMENTAL RESULTS AND DISCUSSION

Fayetteville shale cores from the FL2 and FL3 vertical sections in the Fayetteville shale formation were used to run a series of fracture conductivity experiments. A typical sample underwent three different experimental conditions unpropped, 0.03 lb/ft^2 of 30/70 mesh sand and 0.1 lb/ft^2 of 30/70 mesh sand. The same sample was used for all three experiments unless a large amount of surface crushing occurred during an experiment, or a significant amount of surface fragments were removed.

3.1 Conductivity of Unpropped Fractures

To provide a baseline for each vertical zone a series of unpropped experiments were run indicating if there was an increase or decrease in fracture conductivity once proppant was applied to the surface. The unpropped baseline experiments also provided a way to identify if fracture conductivity within the same zone would behave similarly. Figure 25 shows the results of three unpropped fracture conductivity samples from the FL3. The plot shows that the conductivity measurements are on the same order of magnitude and behave similarly. Figure 26 provides a similar conclusion for the unpropped experiments run for samples in the FL2 zone. The unpropped conductivity measurements in each zone are consistent within that zone; however, the two zones unpropped conductivities are not similar. Figure 27 shows that the unpropped

conductivity of FL3 samples are two orders of magnitude lower than the unpropped conductivity measured from FL2 samples.

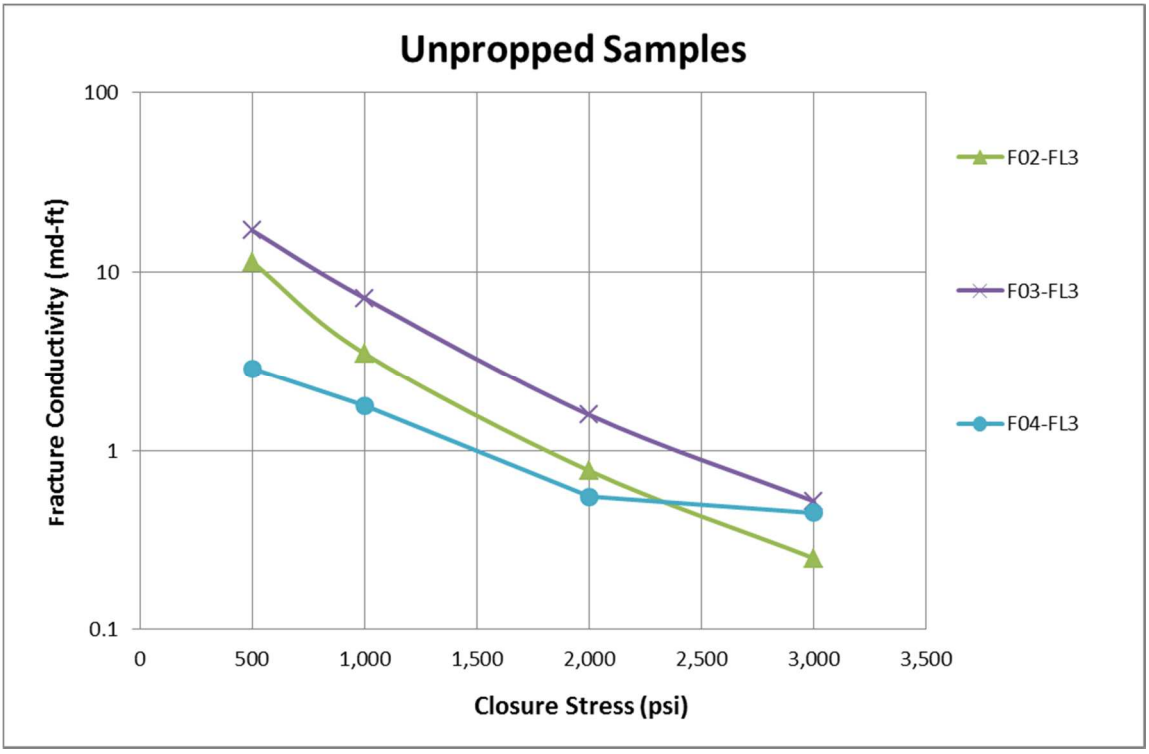

Figure 25 - Unpropped FL3 fracture conductivity

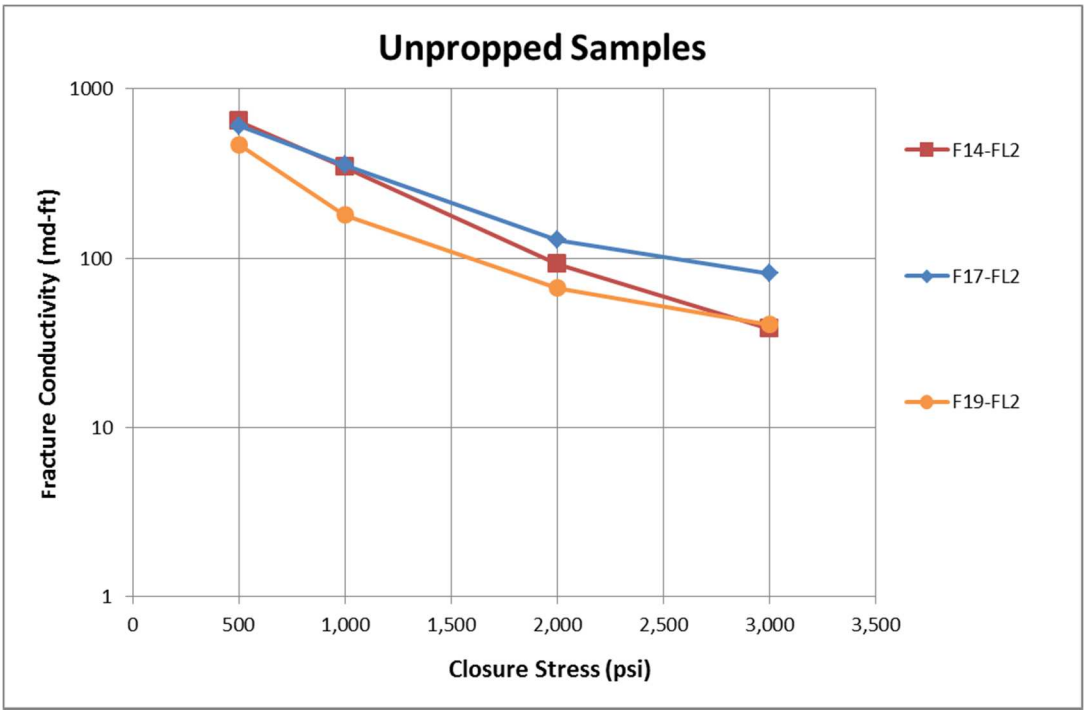

Figure 26 - Unpropped FL2 fracture conductivity

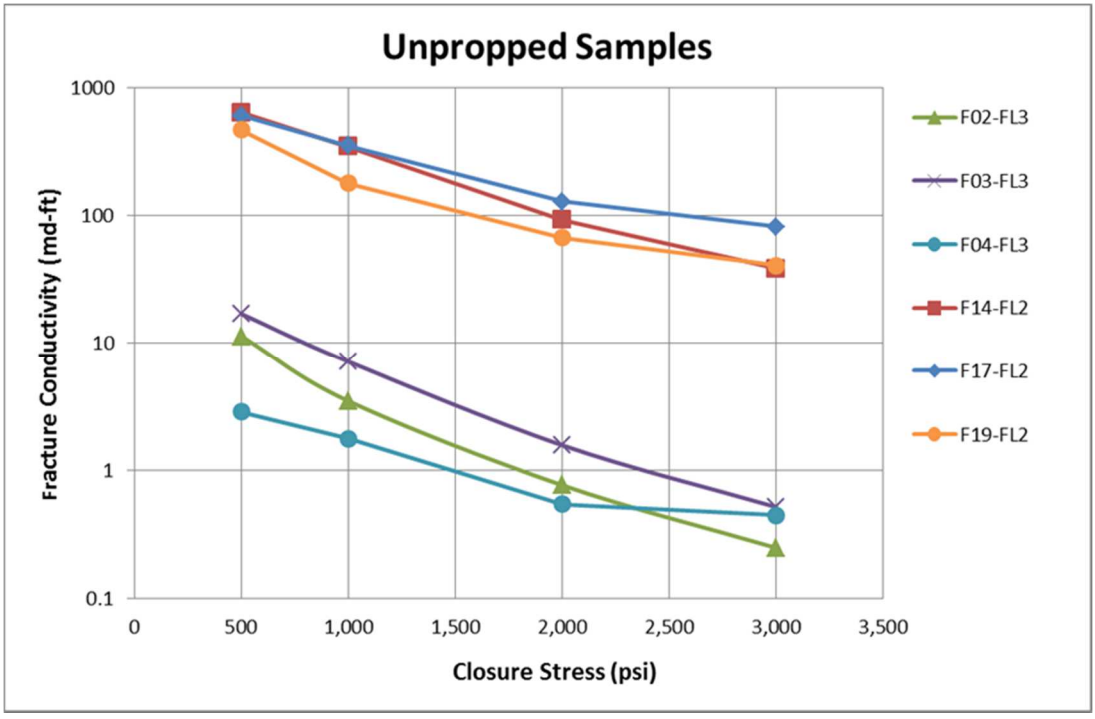

Figure 27 - Unpropped results from the FL2 and FL3

The unpropped fracture conductivity depends significantly on the residual fracture width, the creation of fragments on the fracture surface, and the size of the fragments created on the fracture surface. Although the unpropped fractures mostly likely will be closed after hydraulic fracturing is finished, any disturbance to the fracture surfaces, such as fragments in the fracture or shear displacement, could create a conductive path for flow. This conductivity may not sustain when closure stress is too high.

3.2 Conductivity of Propped Fractures

After the unpropped experiment was complete proppant was evenly distributed on the fracture surface. The proppant selected for this experimental study was 30/70

mesh Arkansas River sand. The proppant concentrations were kept low, 0.03 lb/ft^2 and 0.1 lb/ft^2 to simulate the low concentrations pumped in the field. The maximum closure stress for all samples is 3,000 psi because the true vertical depth of an average well in the Fayetteville shale is approximately 3,700 ft. with an approximate in-situ stress of 0.7 psi/ft (Harpel et al., 2012).

The proppant type, concentrations and size for the experiments in this study were kept the same for each sample to minimize the impact of proppant variation on conductivity. Proppant embedment, rearrangement, crushing etc. were factors that could not be controlled as easily. Flow rates at lower closure stresses were increased slowly and kept as low as possible to try to avoid rearrangement of proppant by gas flow. Figure 28 graphically depicts the unpropped, 0.03 lb/ft^2, and 0.1 lb/ft^2 concentration conductivity results of an FL3 sample. The same graphical depiction can be seen in Figure 29 for a sample in the FL2. Figure 28 and Figure 29 show that placing proppant on the surface will increase the conductivity significantly compared to the unpropped measured conductivity.

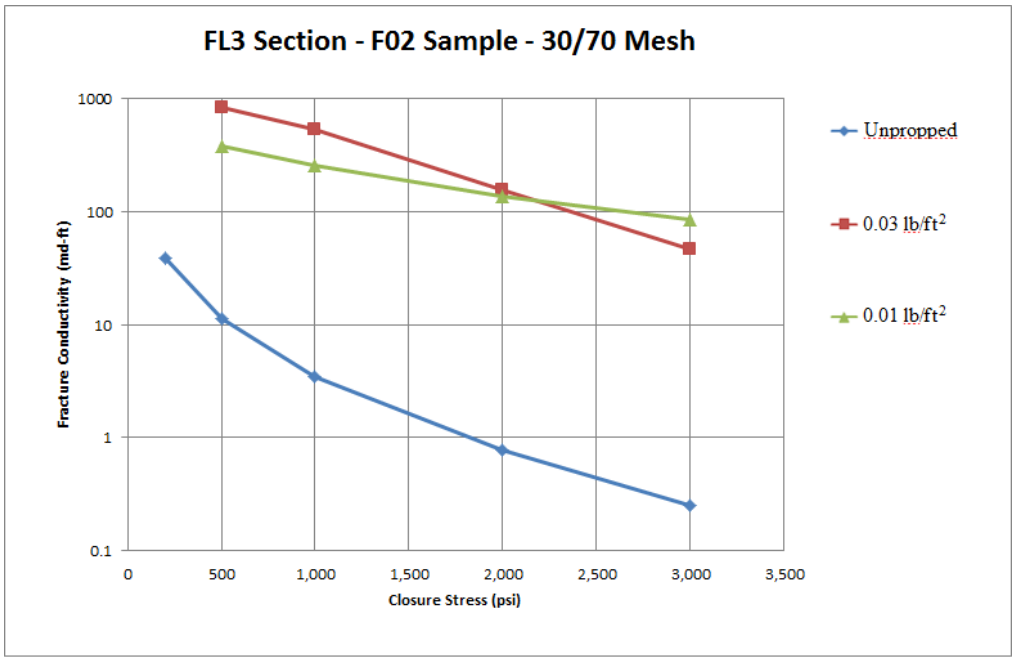

Figure 28 - FL3 sample F02 experimental results

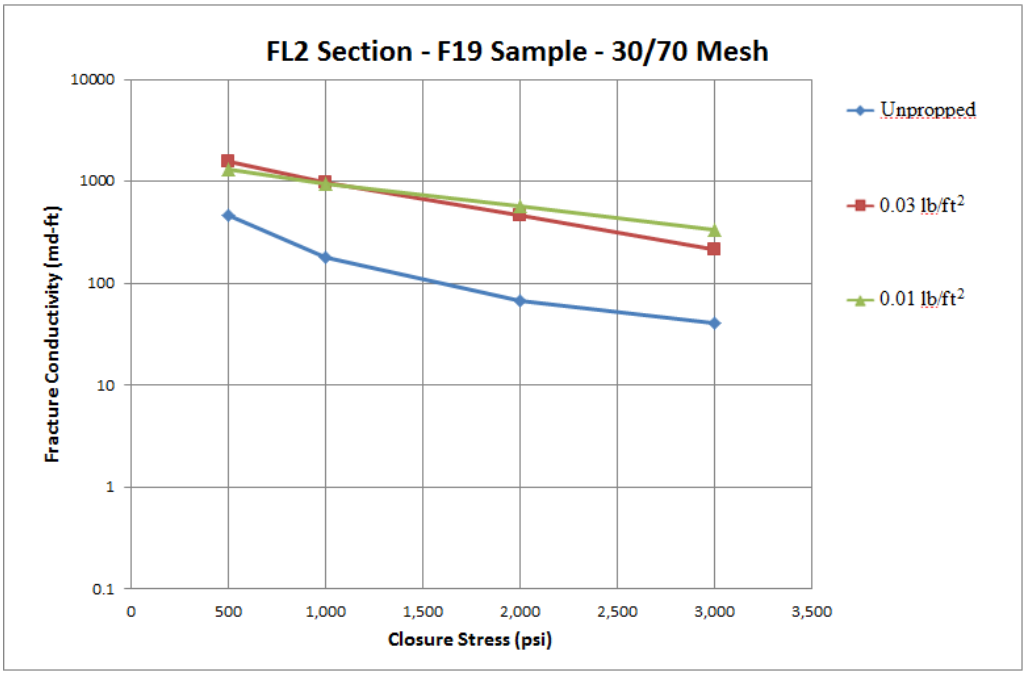

Figure 29 - FL2 sample F19 experimental results

3.2.1 Conductivity Measurements at 0.03 lb/ft^2 Concentration

The experimental results for 0.03 lb/ft^2 concentration of 30/70 mesh sand in both the FL2 and FL3 zones results in a partial-monolayer when the closure stress is below 2,000 psi (Brannon et al., 2004). The decrease in conductivity begins to have a sharper decrease around 1,000 psi, but the initial conductivity at ultra-low closure stresses show that both concentrations maintain similar conductivities. The void space on the fracture surface preventing a full monolayer is shown below in Figure 30. This seems to be a phenomenon at ultra-low closure stress, 500 psi, because the increase in closure stress significantly reduces the conductivity for 0.03 lb/ft^2 concentrations.

Figure 30 - low concentration proppant distribution on a FL3 sample

The results for the FL2 and FL3 samples with 0.03 lb/ft^2 concentration of 30/70 mesh sand vary similarly to what was seen in the unpropped results. However, the conductivity difference between the two zones is less severe than what was seen in the unpropped experiments. The FL3 unpropped experiments were on average less than 1% of the conductivity measured in the upropped FL2 experiments. The FL3 0.03 lb/ft^2 concentration experiments on average are 26% of the measured FL2 experiments under the same conditions. The results from three FL3 and three FL2 0.03 lb/ft^2 concentration experiments can be seen below in Figure 31, where the FL2 conductivities remain higher than the FL3.

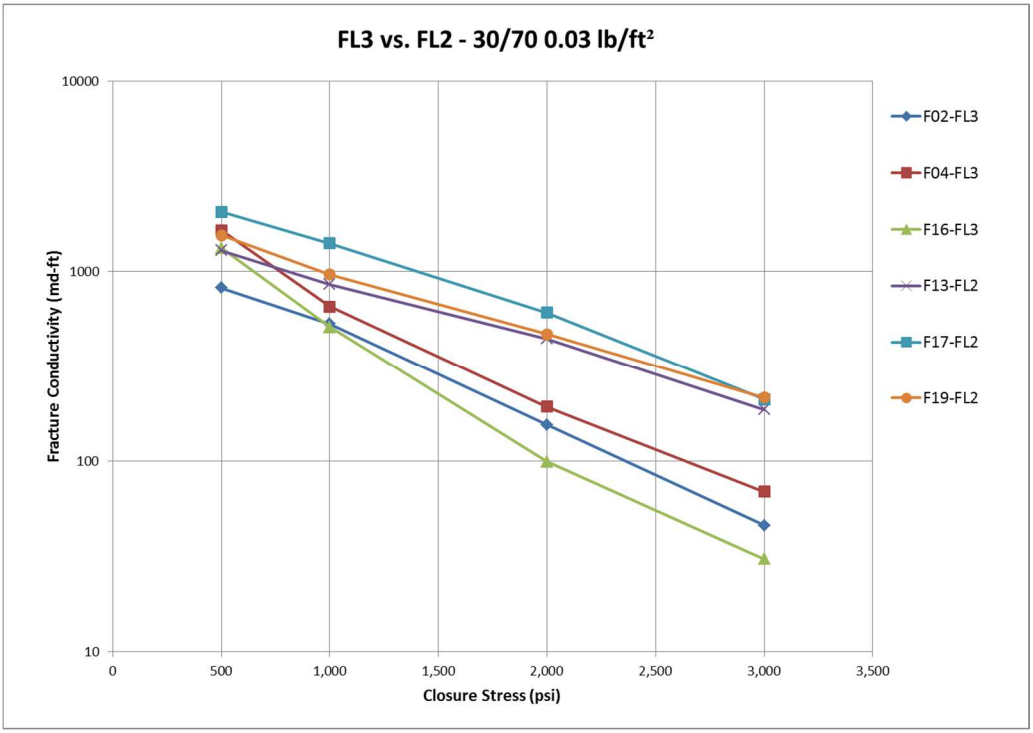

Figure 31 - FL3 and FL2 experimental results at 0.03lb/ft^2

3.2.2 Conductivity Measurements at 0.1 lb/ft^2 Concentration

The final concentration used in this experimental study was 0.1 lb/ft^2 of 30/70 mesh sand. The effect of partial mono-layer seen in the lower concentration of proppant is no longer seen at this concentration level. Additionally, the separation between FL3 conductivity measurements and the FL2 measurements has again decreased. The average FL3 conductivity measurement at 0.1 lb/ft^2 concentration is 33% of the FL2 conductivities under the same conditions. The variation between the FL3 and FL2 conductivity values can be seen below in Figure 32.

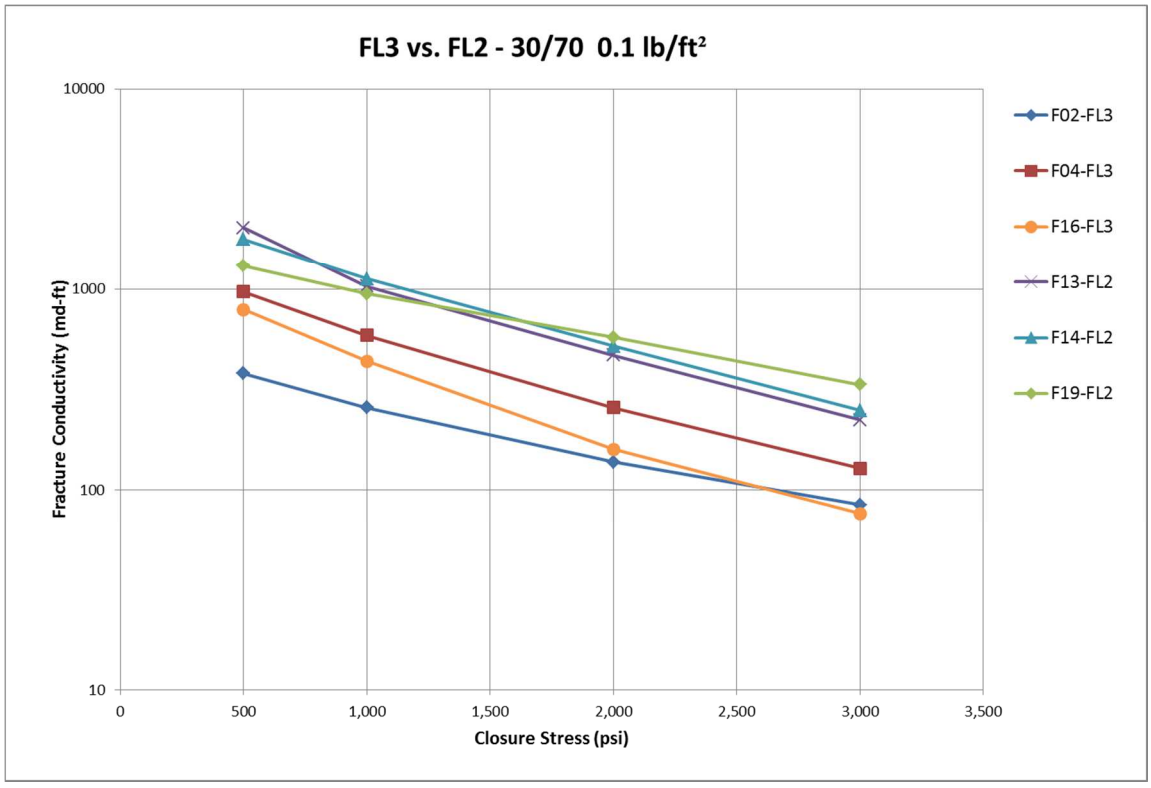

Figure 32 - FL3 and FL2 conductivity measurements results for 0.1 lb/ft^2

3.3 Conductivity Analysis

The FL2 had higher conductivity values in all three experimental conditions. The results of three experiments at each experimental condition were average to provide a means of comparing the FL2 and FL3 zones at each concentration. A plot of the averaged values can be seen in Figure 33. The most noticeable result shown in this plot is the FL3 conductivity increases from unpropped to 0.03 lb/ft^2 concentration. Additionally, the partial mono-layer effect seen at 0.03 lb/ft^2 is most obvious on the FL3 surface. The slope of the 0.03 lb/ft^2 FL3 conductivity is much steeper than the other concentration line slopes. The final difference observed is that FL3 consistently has lower conductivities compared to the FL2.

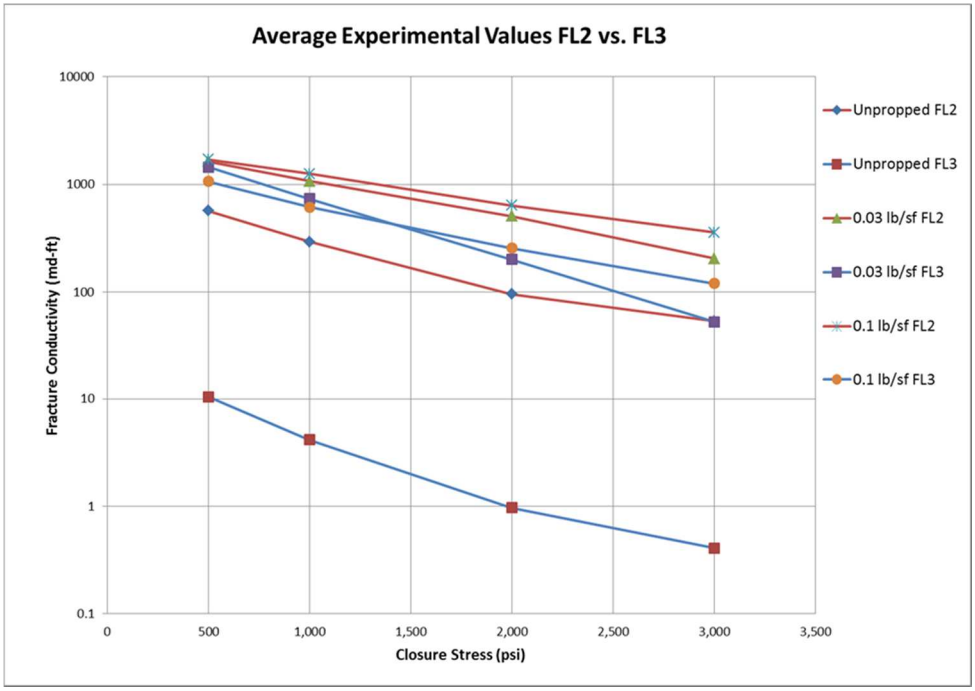

Figure 33 - Graphical representation of average fracture conductivity results

The numerical values from the conductivity results can be seen in Table 3.

Table 3 – Laboratory conductivity measurements

	Average Conductivity at 3,000 psi closure stress with 30/70 mesh proppant		
Fracture Zone	***Unpropped***	***0.03 lb/ft²***	***0.1 lb/ft²***
FL2	53.58	205	359.1
FL3	0.406	52.8	120.2
FL3 Conductivity Percentage of FL2	1%	26%	33%

Table 3 shows clearly that the degree of conductivity separation between the FL2 and FL3 decreases as proppant concentration is increased. The decrease is most noticeable between unpropped conductivity and 0.03 lb/ft^2 concentration conductivity. The FL3 conductivity increases approximately 25% closer to the FL2 conductivity measurement. The FL3 only becomes an additional 7% closer to the FL2 conductivity when changing the concentration from 0.03 lb/ft^2 to 0.1 lb/ft^2.

The difference between the FL2 and FL3 fracture surface fragments are significantly different. Due to the laminated nature of the FL3 fractures the fragments on the surface are flat and flaky. The FL2 surface fragments are bulky, irregular fragments that are larger than that seen on the FL3 surface.

The fracture surface of an FL3 sample has dusty, flaky fragments instead of the larger, bulky fragments seen on the FL2 fracture surface. Dusting off the surface of an FL3 sample results in the loss of particles shown in Figure 34. The penny is used for scale to compare the fragments from the FL3 samples to the fragments from the surface of the FL2. An example of an FL2 sample with surface fragments still on the surface is shown in Figure 35. The size of the surface particles dusted from the fracture surface of the FL2 sample in Figure 35 can be seen in Figure 36. The particles dusted from the FL2 sample are much larger and bulkier relative to the flaky fragments dusted off the FL3 fracture surface. When the fracture surface breaks or crushes during an experiment, resulting in unusable conductivity data, the broken particles are similar to the surface fragments created during fracturing, but on a larger scale as shown in Figure 37 and Figure 38.

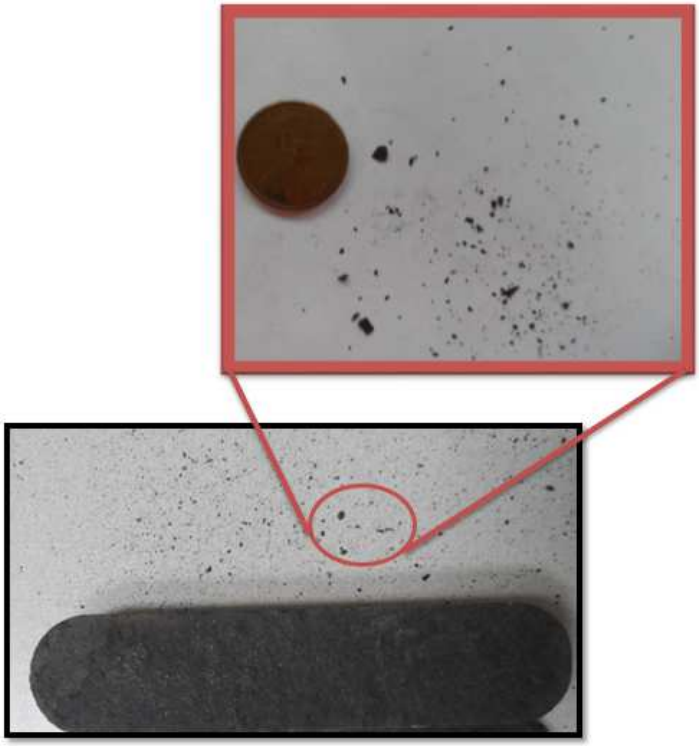

Figure 34 - FL3 fracture surface particle size

Figure 35 - FL2 fracture surface with fragments

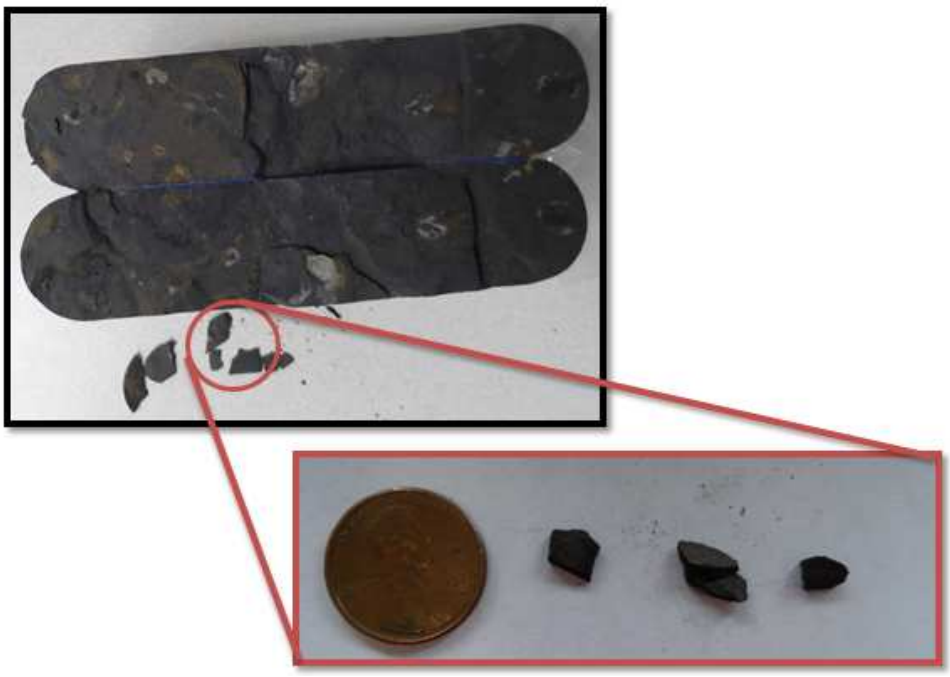

Figure 36 - FL2 fracture surface particle size

Figure 37 shows the fracture surface of an FL2 sample after a 0.03 lb/ft^2 concentration experiments. The surface crushed during the experiment possibly causing inaccurate conductivity measurements; therefore, this experimental data was not used and the sample was not used for any more experiments. The FL2 samples in this work required extra attention and care to keep the fracture surface from crushing. Many experiments were lost due to crushing or lack of fracture surface integrity. The difference in surface fragments and particles from a crushed sample can be seen in Figure 37. The crushed surface has much larger fragments, and if fragments were removed the alignment of the fracture surfaces would be greatly affected. For this reason many samples were compromised after one or two experiments. The fragile nature of the FL2 may have a

contribution to high conductivity, possible fracture network, and therefore higher production after stimulation.

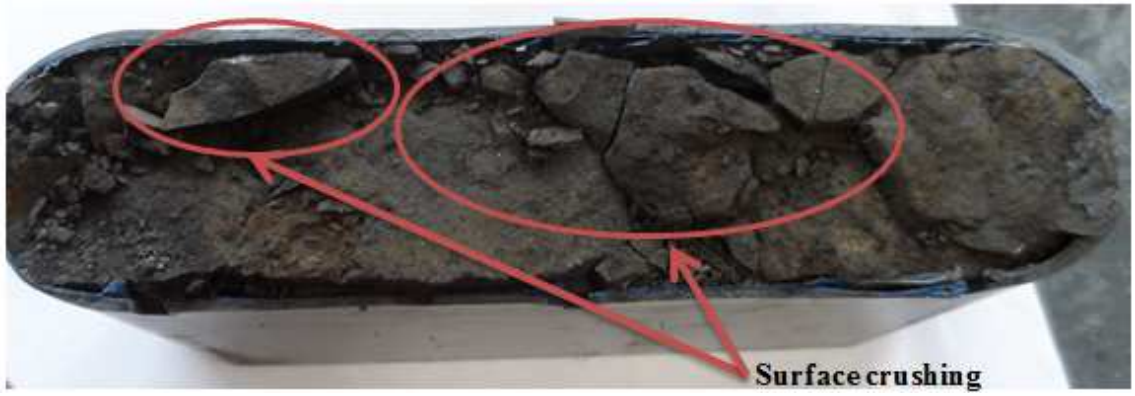

Figure 37 - FL2 crushed fracture surface

The FL3 samples on the other hand broke less on the fracture surface and more throughout the sample itself. Typical sample failure in the FL3 consisted of breakage along planes parallel to the fracture surface shown in Figure 38. Fracture surface integrity was much easier to maintain with FL3 samples and multiple experiments were conducted on each sample. Due to the laminar, flat nature of the FL3 fracture surface, when the samples are fractured the surface particles are flaky, flat as seen in Figure 34.

Figure 38 - FL3 crushed sample

The fracture surface, void space, and particle size become less of a factor as more proppant is placed on the surface. Although both fracture surfaces produce surface fragments, the flat, flaky nature of the FL3 surface fragments do not have as significant of an impact to fracture conductivity as the bulky, blocky fragments created on the FL2 surface. On an unpropped surface the slightest realignment of surface particles in the FL2 can create a path for gas to flow resulting in higher conductivity values. On the other hand the slightest realignment of a fragment on the FL3 surface may allow conductivity at ultra-low closure stresses, such as, 500 psi, but as the closure stress increase to 3,000 psi these fragments are crushed or align flat enough with the flat fracture surface that they do not greatly impact the conductivity. As the proppant concentration is increased the degree of influence these surface fragments and void spaces have on the fracture conductivity reduces. However, the FL2 consistently has

higher conductivities than the FL3, suggesting that the surface fragment size combined with void spaces and fracture roughness will create conductivities higher than a flat, laminated fracture surface with weak, flaky surface fragments.

3.4 Vertical Zone Variations

The primary objective of this work was to compare laboratory conductivity results from the FL2 and FL3 vertical sections of the Fayetteville shale; however, understanding the geological and production differences can provide supporting evidence the conductivity analysis. Production data analysis provides insight into the possibility of observing conductivity measurement differences because production is closely related to conductivity of fractures. Rock properties have been discussed in many pieces of literature as a factor effecting fracture conductivity. Understanding these two topics could paint a better picture of what to expect from laboratory conductivity measurements.

Southwestern Energy provided 90-day cumulative production data for wells that were 100% within the FL2 and FL3 and located in the same area of the field. Additionally, x-ray diffraction and thin section analysis was used to see if there was any geological differences. The 90-day production data was compared with the completions design to normalize the data because each wellbore had different length, number of stages, number of clusters and number of perforations. Figure 39 depicts a typical horizontal wellbore within the Fayetteville shale (Harpel et al., 2012).

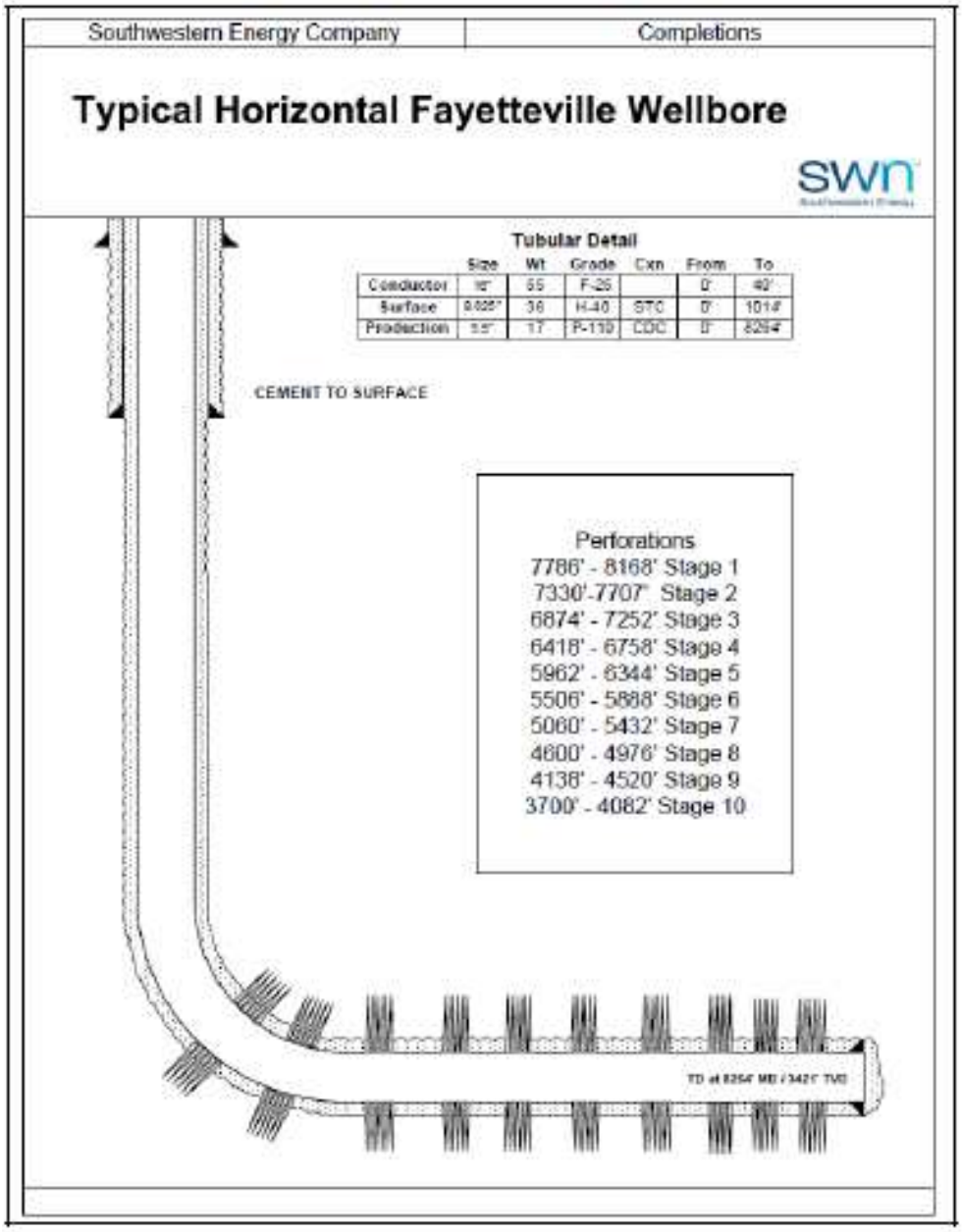

Figure 39 - Schematic of a typical horizontal wellbore in the Fayetteville shale

Evaluating the schematic design of a typical horizontal wellbore in the Fayetteville shale, the 90-day production was normalized by dividing by the number of perforations because the perforations are the first channel of communication to the formation. The data should not be normalized by completed lateral length because the number of stages, clusters, and perforations can be different from well to well. Additionally, the data should not be analyzed by stage or cluster because the amount of perforations per cluster may vary from well to well. For these reasons the number of perforations is the best way to normalize the data because they cannot be further broken down into another variable. Table 4 analyzes the 90-day cumulative production data from four well pad locations. One well at each location was drilled and completed in the FL3 and is compared to one or two wells drilled and completed in the FL2. Analysis of data in Table 4 concludes that a wellbore placed in the FL3 will produce approximately 1/3 the production of a wellbore placed in the FL2.

Table 4 - Production data anaylsis from the FL2 and FL3

Well Site Location	Well Number	Zone	Percentage in Zone	90 day Cumm	Average Concentration (ppg)	CLAT	Total Perforations	Cumm/Perforation	FL3 Production as % of FL2
1	1	3	100%	136,570.40	0.69	5,055	703	194.27	
1	2	2	100%	310,589.90	0.76	5,397	528	588.24	33%
1	3	2	100%	273,982.10	0.97	4,276	432	634.22	31%
2	1	3	100%	31,245.60	0.76	4,430	498	62.74	
2	2	2	91.60%	105,459.80	0.76	5,137	528	199.73	31%
3	1	3	93.50%	59,137.00	0.70	3,995	450	131.42	
3	2	2	98.40%	234,090.02	0.76	5,058	558	419.52	31%
3	3	2	100%	198,495.38	0.76	5,122	518	383.20	34%
4	1	3	100%	100,015.00	0.70	4,322	550	181.85	
4	2	2	75.20%	299,416.00	0.70	4,486	528	567.08	32%

In addition to production data, rock properties in the FL2 and FL3 were also compared by surface scans, x-ray diffraction analysis and thin section analysis. A surface scan of a sample's fracture surface was measured after the unpropped experiment, but before the propped experiments. Figure 40 and Figure 41 show the results of the laser profilometer scans from an FL2 and FL3 sample, respectively.

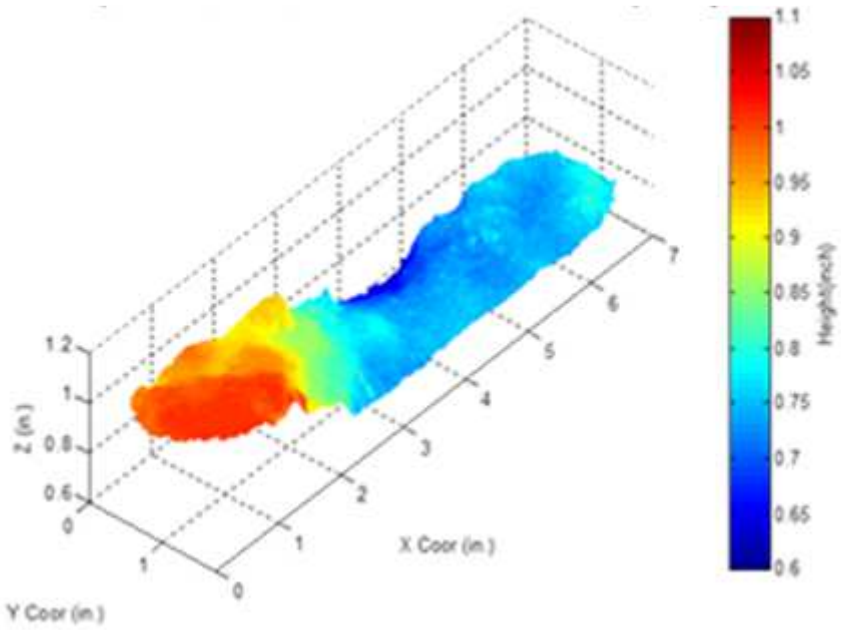

Figure 40 - FL2 laser profilometer fracture surface scan

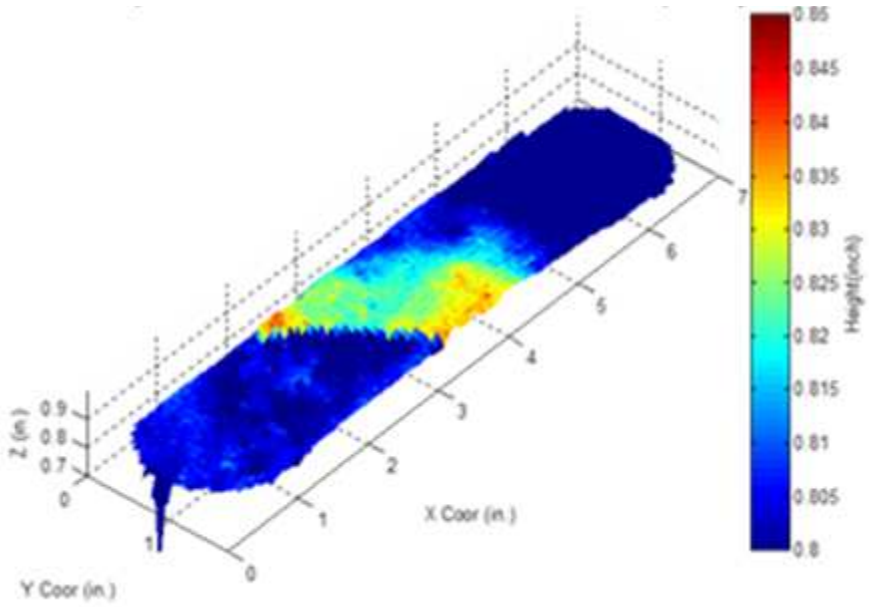

Figure 41 - FL3 laser profilometer fracture surface scan

The fracture surface of the FL3 varies a total of 0.05 in. whereas the FL2 sample varies by 0.5 in. The FL3 is highly laminated shale that fractures parallel to the laminated planes resulting in flatter fracture surfaces. The FL2 on the other hand does not have a defined fracture plane or pattern resulting in rough fracture surface.

Thin section analysis was further investigated at the bedding planes and natural fractures in the FL2 and FL3. Figure 42 and Figure 43 show a thin section cut perpendicular to the FL2 and FL3 samples fracture surface, respectively. The grain size of the FL2 is much smaller than that in the FL3 sample. Additionally, there is noticeable difference in the natural facture orientation. The FL3 sample in Figure 43 shows three parallel natural fractures. These natural fractures are occurring parallel to the laminated plane. In contrast, the FL2 sample in Figure 42 does not show evidence of planar fractures. Fracture direction is predominately horizontal or in the orientation of bedding,

but the fracture varies vertically as well resulting in a fracture that is not a straight line fracture. The fracture surface variability shown in the profilometer surface scans is supported by the natural fracture orientation in the thin sections.

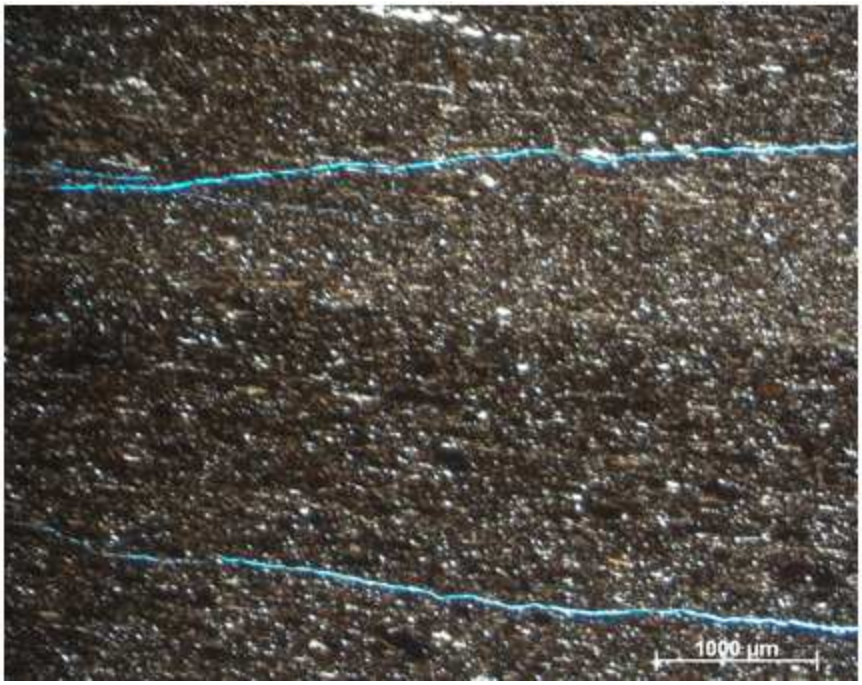

Figure 42 - FL2 thin section analysis

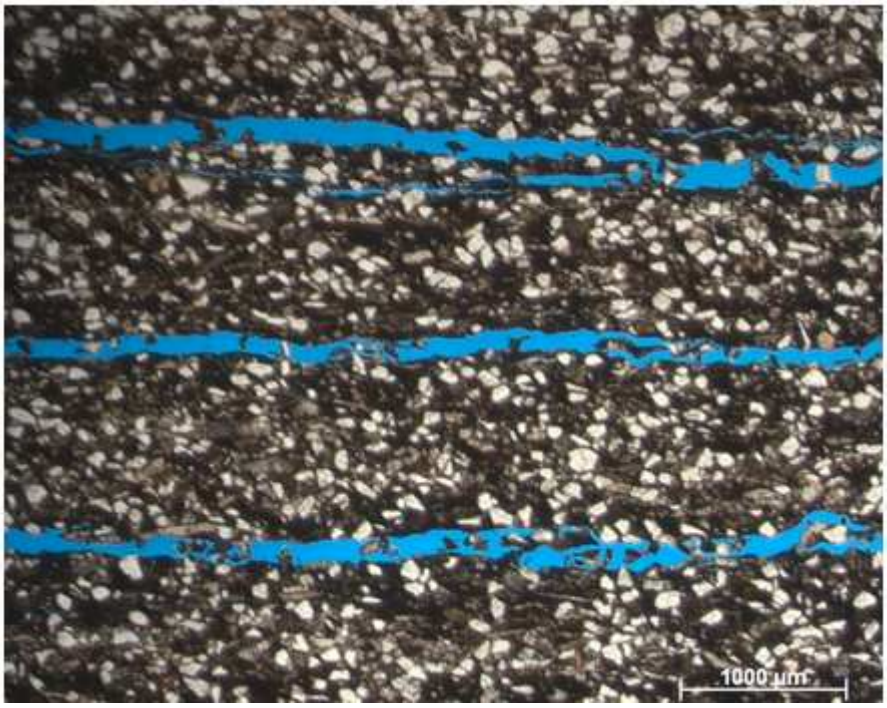

Figure 43 - FL3 thin section analysis

The final analysis of the rock properties was mineralogical analysis. To determine the mineralogical make up of both zones x-ray diffraction and Fourier transform infrared spectroscopy of 9 samples was outsourced for analysis. The results of this data are shown below in Table 5. The FL2 and FL3 yet again have noticeable differences. The FL2 is dominated by clay and quartz, whereas the FL3 mineral content is evenly distributed between clay, carbonate and quartz.

Table 5 - Mineralogical data

Well	Sample Number	Analysis Type	Mineralogy			
			Clays	Carbonate	Quartz	Feldspar
Fayetteville - FL 2	9	FTIR	39	2	54	5
Fayetteville - FL 2	10	FTIR	37	1	57	5
Fayetteville - FL 2	11	FTIR	34	4	57	5
Fayetteville - FL 3	3	FTIR	36	1	57	6
Fayetteville - FL 3	4	FTIR	35	28	35	2
Fayetteville - FL 3	5	FTIR	34	31	33	2
Fayetteville - FL 3	6	FTIR	38	28	32	2
Fayetteville	Fl- 2	XRD	42	0	55	3
Fayetteville	FL - 3	XRD	10	38	50	2

The analysis of fracture surface scans, thin sections and x-ray diffraction from samples in the FL2 and FL3 suggests that there will be variability in conductivity measurements if rock property differences can be identified between zones. Additionally, from evaluating the 90-day cumulative production data, wells in the FL3 produces less than wells in the FL2. Given that well production is influenced by fracture conductivity, the production data provides evidence that the FL3 should have lower conductivity than the FL2.

4. CONCLUSIONS AND RECOMMENDATIONS

4.1 Conclusions

In conclusion, this study evaluated the differences between two different vertical zones, the FL2 and FL3, within the Fayetteville shale formation. The primary goal of this work was to investigate laboratory fracture conductivity measurements from the FL2 and FL3.

To better understand the rocks used in this work rock property and production analysis methods were used. The first method of understanding the differences in the two zones was analyzing 90-day cumulative production data provided by Southwestern Energy. The 90-day production data was compared by normalizing the cumulative production per the total number of perforations in the wellbore. The production data analysis concluded that wellbores placed predominately in the FL3 produced approximately 30% of what a well placed in the FL2 within the same location produced. The second method used to distinguish the differences between the zones was rock fracture surface profilometer scans. The scans indicated that the FL2 fracture surface did not break in a planar fashion and the FL3 fracture surface broke flat along a laminated plane. The third method of understand how these two zones differed was by looking at thin sections cut perpendicular to the rock fracture surface. The thin sections provided insight that natural fractures in the FL2 did not follow a parallel plane, whereas the natural fractures in the FL3 preferred to break along parallel, laminated planes. The final method used to distinguish zonal differences was analysis of mineral composition

using x-ray diffraction. The mineral composition analysis concluded that the FL2 and FL3 samples had similar clay content, but the FL2 contained more quartz and the FL3 contained more carbonate. The results from the rock property and production analysis provided evidence that the two zones fracture conductivity measurements should be different if fracture conductivity is influenced by the rock parameters measured.

Laboratory fracture conductivity results confirmed that the two zones had different conductivities. The following conclusions and observations were made based on the fracture conductivity experimental study:

1. Unpropped fracture conductivity in the FL2 is two orders of magnitude larger than the unpropped conductivity in the FL3.
2. Perfectly aligned unpropped fracture conductivity measurements in the FL2 and FL3 can be greatly affected by misalignment of bulky surface fragments up to 3,000 psi closure stress (formation in-situ stress gradient). Void space created by relocation of bulky surface particles can create high conductivity pathways.
3. Perfectly aligned unpropped fracture conductivity measurements in the FL2 and FL3 are not significantly affected by flaky, brittle surface fragments up to 3,000 psi closure stress (formation in-situ stress gradient).

4. Propped fracture conductivity reduces the severity of zonal fracture conductivity difference. The unpropped FL3 fracture conductivity is 1% of the unpropped fracture conductivity in the FL2. Applying 0.03 lb/ft^2 concentration of 30/70 mesh proppant decreases the degree of difference. The FL3 fracture conductivity becomes 26% of the FL2 fracture conductivity. Increasing the proppant concentration to 0.1 lb/ft^2 only changes the degree of difference by 7% resulting in the FL3 fracture conductivity becoming 33% of the FL2 fracture conductivity.
5. Fracture conductivity increases with proppant concentration for low proppant concentration applications (0.03 lb/ft^2 and 0.1 lb/ft^2).
6. The size and brittleness of surface fracture particles significantly impacts the unpropped and low concention fracture conductivity.
7. The FL2 zone of the Fayetteville shale is a much more conductive zone relative to the FL3 zone. Analysis of 90-day cumulative production provides supporting evidence concluding that the FL3 production on average is approximately 1/3 the production of the FL2.

4.2 Recommendations

Moving forward investigation of rock properties should be performed to evaluate the cause of non-planar fractures. Additionally, the short-term shale fracture conductivity experiments performed in this study used dry nitrogen on surfaces that had not been exposed to liquid. Southwestern Energy is the primary operator in the

Fayetteville shale and are currently fracturing using a slick-water fracturing fluid with scale inhibitors, friction reducers and biocide additives. Future work should investigate long-term dynamic conductivity measurements using fracturing fluid similar to what is pumped in the Fayetteville shale. This evaluation would help understand whether liquid contact with fracture surfaces can reduce the zonal conductivity differences in unpropped and low concentration cases.

REFERENCES

Brannon, H. D., Rickards, A. R., Wood, W. D., Edgeman, J. R., Bryant, J. L. (2004). Maximizing Fracture Conductivity with Proppant Partial Monolayers: Theoretical Curiosity or Highly Productive Reality? *SPE Annual Technical Conference and Exhibition.* Houston.

Gidley, J. L., Holditch, S. A., Nierode, D. E., Veatch Jr., R. W. (1989). *Recent Advances in Hydraulic Fracturing.* Richardson, TX: Society of Petroleum Engineers, Inc.

Glorioso, J. C., Rattia, A. J. (2012). Unconventional Reservoirs: Basic Petrophysical Concepts for Shale Gas. *SPE/EAGE European Unconventional Resources Conference and Exhibition.* Vienna, Austria: Society of Petroleum Engineers, Inc.

Harpel, J., Barker, L., Fontenot, J., Carroll, C., Thomson, S., Olson, K. (2012). Case History of the Fayetteville Shale Completions. *SPE Hydraulic Fracturing Technology Conference.* The Woodlands, TX: Society of Petroleum Engineers.

Hill, A. D., Zhu, D., Zhang, J., Kamenov, A. (2013). Laboratory Measurement of Hydraulic Fracture Conductiities in the Barnett Shale. *International Petroleum Technology Conference.* Beijing, China: Society of Petroleum Engineers.

Ispas, I., Stanchits, S., Burghardt, J., Suarez-Rivera, R., Lopez, H., Surdi, A. (2013). Understanding The Effect of Rock Fabric on Fracture Complexity For Improving Completion Design and Well Proformance. *International Petroleum Technology Conference.* Beijing, China: Society of Petroleum Engineers.

Jones, J. R., Britt, L. K. (2009). *Design and Appraisal of Hydraulic Fractures.* Richardson, TX: Society of Petroleum Engineers, Inc.

Ketter, A. A., Heinze, J. R., Daniels, J. L., Waters, G. (2008, August). A Field Study in Optimizing Completion Strategies for Fracture Initiation in Barnett Shale Horizontal Wells. *SPE Production & Operations, 23*(3), 373-378.

Knackstedt, M., Kelly, J., Saadatfar, M., Senden, T., Sok, R. (2005). Rock Fabric and Texture From Digital Core Analysis. *SPWLA 46th Annual Logging Symposium.* New Orleans, LA: Society of Petrophysicists and Well Log Analysts.

Matthews, H. L., Schein, G. W., Malone, M. (2007). Stimulation of Gas Shales: They're All the Same Right? *SPE Hydraulic Fracturing Technology Conference.* College Station, TX: Society of Petroleum Engineers.

Mayerhofer, M. J., Richardson, M. F., Walker Jr., R. N., Meehan, D. N., Oehler, M. W., Browning Jr., R. R. (1997). Proppants? We Don't Need No Proppants. *Annual Technical Conference and Exhibition.* San Antonio, TX: Society of Petroleum Engineers.

Palisch, T. T., Duenckel, R. J., Bazan, L. W., Heidt, J. H., Turk, G. A. (2007). Determining Realistic Fracture Conductivity and Understanding its Impact on Well Performance - Theory and Field Examples . *SPE Hydraulic Fracturing Technology Conference.* College Station, TX: Society of Petroleum Engineers.

Torres-Verdin, C., Adiguna, H. (2013). Comparative Study for the Interpretation of Mineral Concentrations, Total Porosity, and TOC in Hydrocarbon-Bearing Shale from Conventional Well Logs. *SPE Annual Technical Conference and Exhibition.* New Orleans, LA: Society of Petroleum Engineers.

van Dam, D. B., de Pater, C. J. (2001). Roughness of Hydraulic Fractures: Importance of In-Situ Stress and Tip Process. *SPE Annual Technical Conference and Exhibition.* Houston, TX: Society of Petroleum Engineers.